Physics – Uspekhi **39** (11) 1109 – 1135 (1996)

REVIEWS OF TOPICAL PROBLEMS PACS numbers: **42.25.–p**, 42.65.Pc, 42.79.Ta, 42.81.Gs

Experimental observation of the optical self-switching of unidirectional distributively coupled waves

A A Maĭer

Contents

Abstract. Theoretical fundamentals of the phenomenon of optical self-switching of unidirectional distributively coupled waves (UDCW) with the linear coupling coefficient have been given in Ref. [1]. The present review deals with experimental examination of this striking phenomenon and pulse self-switching events along with the theory of UDCW self-switching in the case of a nonlinear coupling coefficient.

1. Introduction

The phenomenon of self-switching of unidirectional distributively coupled waves (UDCW) with a linear coupling coefficient was theoretically examined at length in Ref. [1]. Figure 1 illustrates this phenomenon in the simplest case of identical waves and presence only one of them at the system input.

There exists a wide class of UDCWs in the integrated [2 – 8], fibre [9 – 11] and nonlinear [12 – 15] optics between which the energy exchange occurs as they are propagating. To these waves one can attribute waves in tunnel-coupled optical waveguides (TCOW), waves with various polarizations in a birefringent crystal or waveguide, waves undergoing the Bragg diffraction in a periodical structure, various modes in the nonuniform waveguide, waves with different frequencies in a quadratically nonlinear medium, etc. The latter possess a nonlinear coupling coefficient, whereas the rest — a linear one.

A A Maĭer General Physics Institute, Russian Academy of Sciences, ul. Vavilova 38, 117942 Moscow, Russia
Tel. (7-095) 132 83 91
Fax (7-095) 135 02 70

Received 15 April 1996, revised 26 August 1996
Uspekhi Fizicheskikh Nauk **166** (11) 1171 – 1196 (1996)
Translated by A Radzig

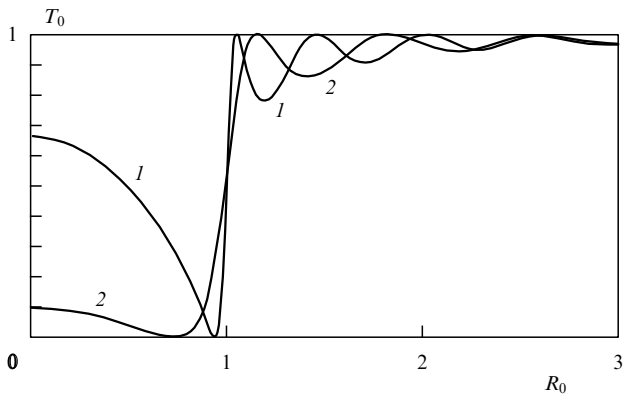

Figure 1. Plots of $T_0 = I_{0l}/I_{00}$ versus $R_0 \equiv I_{00}/I_{0M}$ at $L = 2\pi Kl/\lambda\beta = 1.6\pi$ (*1*) and 1.2π (*2*); UDCWs are identical and only a zeroth wave arrives at the system input.

It should be emphasized that the UDCW class is wider than that of waves with oppositely directed coupled waves used for producing the optical bistable switches [16 – 32]. The theory of linear interaction between UDCWs with a linear coupling coefficient has long been developed in detail [2 – 11].

The author was the first to reveal in Refs [33 – 35]† that in the nonlinear regime the UDCW self-switching can occur in certain conditions. The phenomenon of interest implies that a small variation of the input intensity for one of the UDCWs gives rise to an abrupt change in the UDCW intensities ratio at the system output. The practical value lies here in the fact that earlier unknown class of optical transistors with record response time has been proposed [33, 34] on the basis of this effect. The latter and some problems related to it were investigated by the author and his coworkers in Refs [33 – 35, 37 – 73] and by other researchers in Refs [36, 74 – 114]. References, as a rule, are arranged in what follows in the chronological order; sometimes they were grouped with due regard for closeness of questions discussed (e.g., [105 – 116]).

The present review article deals with experiments on examination of UDCW self-switching in the case of linear wave-coupling coefficients and with theoretical consideration of UDCW self-switching in the quadratically nonlinear medium for the case of a nonlinear wave-coupling coefficient. What is more, we will concern with the pulse self-switching as just the latter has been observed in the first experiments [45, 46] (by virtue of the fact that rather high input intensities are required in its observing). It would be a good thing to compare also the theoretical prediction of the pulse-shape change in the process of their self-switching with that found in the experiment.

2. Reshaping the bell-shape pulse in its self-switching

Let us consider the problem of shape variation of the bell-shape laser pulse in its passage through the system with UDCWs (in the case of a linear wave-coupling coefficient) characterized by the intensity-dependent refraction index.

2.1 On the equations

The behaviour of the pulse in the system with UDCWs propagating through the cubically nonlinear medium (and with allowance made for dispersion as well as delayed nonlinear response, nonlinear dispersion of group velocity, and coupling coefficient dispersion) can be described by the equations [69]:

$$2\mathrm{i}\left(\frac{\partial a_0}{\partial z_\mathrm{n}}+v\,\frac{\partial a_0}{\partial \tau_\mathrm{n}}\right)+D_\mathrm{n}\frac{\partial^2 a_0}{\partial \tau_\mathrm{n}^2}-\mathrm{i}\mu_3\frac{\partial^3 a_0}{\partial \tau_\mathrm{n}^3}=-L\Bigg\{a_1\exp(\mathrm{i}z_\mathrm{n}\xi L)+\mathrm{i}\mu_K\frac{\partial a_1}{\partial \tau_\mathrm{n}}\exp(\mathrm{i}z_\mathrm{n}\xi L)+4\Bigg[\Theta_{0\mathrm{n}}|a_0|^2a_0+\Theta_{01\mathrm{n}}|a_1|^2a_0+\widetilde{\Theta}_\mathrm{n}a_1^2a_0^*\exp(2\mathrm{i}z_\mathrm{n}\xi L)-\mu a_0\frac{\partial|a_0|^2}{\partial\tau_\mathrm{n}}-\mathrm{i}\mu_\mathrm{n}\frac{\partial}{\partial\tau_\mathrm{n}}\left(|a_0|^2a_0\right)\Bigg]\Bigg\},$$

$$2\mathrm{i}\left(\frac{\partial a_1}{\partial z_\mathrm{n}}-v\,\frac{\partial a_1}{\partial \tau_\mathrm{n}}\right)+D_\mathrm{n}\frac{\partial^2 a_1}{\partial \tau_\mathrm{n}^2}-\mathrm{i}\mu_3\frac{\partial^3 a_1}{\partial \tau_\mathrm{n}^3}=-L\Bigg\{a_0\exp(-\mathrm{i}z_\mathrm{n}\xi L)+\mathrm{i}\mu_K\frac{\partial a_0}{\partial \tau_\mathrm{n}}\exp(-\mathrm{i}z_\mathrm{n}\xi L)+4\Bigg[\Theta_{1\mathrm{n}}|a_1|^2a_1+\Theta_{10\mathrm{n}}|a_0|^2a_1+\widetilde{\Theta}_\mathrm{n}a_0^2a_1^*\exp(-2\mathrm{i}z_\mathrm{n}\xi L)-\mu a_1\frac{\partial|a_1|^2}{\partial\tau_\mathrm{n}}-\mathrm{i}\mu_\mathrm{n}\frac{\partial}{\partial\tau_\mathrm{n}}\left(|a_1|^2a_1\right)\Bigg]\Bigg\},\tag{2.1.1}$$

where $L=2\pi Kl/\beta\lambda$; $K=\beta\lambda/(2l_\mathrm{c})$ is the linear wave-distributed coupling coefficient; l is the system length; l_c is the coupling length in the linear regime at $\xi=v=D_\mathrm{n}=\mu=\mu_\mathrm{n}=\mu_K=\mu_3=0$, i.e. the length of a power transfer; λ is the wavelength; $\Theta_{j\mathrm{n}}=\Theta_j/|\Theta|$, $\Theta_{10\mathrm{n}}=\Theta_{01\mathrm{n}}=\Theta_{01}/|\Theta|$, and $\widetilde{\Theta}_\mathrm{n}=\widetilde{\Theta}/|\Theta|$ are the normalized nonlinear coefficients; $\Theta=(\Theta_0+\Theta_1)/2$, Θ_j, $\Theta_{01}=\Theta_{10}$, and $\widetilde{\Theta}$ are the nonlinear coefficients of wavequides [1, 34]. If UDCWs are the waves in TCOW or modes of different order in a separate waveguide, then usually $|\Theta_{10}|\ll|\Theta|$ and the cross terms involving $\Theta_{10\mathrm{n}}$ and $\widetilde{\Theta}_\mathrm{n}$ coefficients, as a rule, can be neglected. The term with $\widetilde{\Theta}_\mathrm{n}$ is significant if by '0' and '1' waves are meant UDCWs of orthogonal polarizations in the birefringent waveguide. In this case $\Theta_{01\mathrm{n}}=2/3$, $\widetilde{\Theta}_\mathrm{n}=1/3$ (see [1, 72]). For the rest of UDCWs, among them waves in TCOW, we may consider that $\widetilde{\Theta}=0$. In addition, $a_j=A_j/\sqrt{I_{0\mathrm{M}}}$ are the normalized wave amplitudes; $I_{0\mathrm{M}}=4K/|\Theta|$ is the critical intensity (of complete self-switching) [1] and it is assumed below that $I_{0\mathrm{M}}=I_\mathrm{M}$ (see [1]); $z_\mathrm{n}=z/l$; $D_\mathrm{n}=Dl/\tau_\mathrm{p}^2$, where $D=\partial^2(\beta\omega/c)/\partial\omega^2$ is the dispersion coefficient; $\mu_3=(l\tau_\mathrm{p}^{-3}/3)\,\partial^3(\beta\omega/c)/\partial\omega^3$ is the third-order dispersion coefficient; $\tau_\mathrm{n}=\tau/\tau_\mathrm{p}$, where τ_p is the pulse length and $\tau=t-z/u$; $v=l\tau_\mathrm{p}^{-1}(u_0^{-1}-u_1^{-1})/2$; $u=2u_0u_1/(u_0+u_1)$ is the mean group velocity; $\xi=\alpha\beta/K$, $\alpha=\beta_1-\beta_0$, β_j is the effective index of refraction for the jth wave ($j=0,1$); $\beta=(\beta_1+\beta_2)/2$; $u_j=\partial\omega/\partial(\beta_j\omega/c)$ is the group velocity of the jth wave; $\mu\simeq T_{nl}/\tau_\mathrm{p}$ accounts for the nonlinearity inertia [15]; $\mu_\mathrm{n}\simeq\tau_\mathrm{p}^{-1}(T_0/\pi-\Theta^{-1}\,\partial\Theta/\partial\omega)$ takes account of the wave nonstationarity and nonlinearity dispersion [15]; $\mu_K\simeq(2K/\omega+\partial K/\partial\omega)(K\tau_\mathrm{p})^{-1}$ allows for the wave nonstationarity and dispersion of the coupling coefficient; T_0 is the period of the optical oscillation, and, finally, T_{nl} is the time of Θ relaxation. We have presented in Ref. [1] the nonlinear waveguide coefficients expressed through the waveguide-mode overlap integrals and $\widehat{\Theta}$-tensor components describing the cubically nonlinear media. As shown, the tensor of isotropic medium may be generally employed for $\widehat{\Theta}$. The distinction between coefficients D_n, μ, μ_n, μ_3, and μ_K for the '0' and '1' waves is neglected, though it can be easily taken into consideration. For this purpose, it will suffice to provide these coefficients with the additional index $j=0,1$.

Energy of the pulse

$$I=\int_{-\infty}^{\infty}\left(|A_0|^2+|A_1|^2\right)\mathrm{d}\tau_\mathrm{n}\tag{2.1.2}$$

is conserved along the system coordinate: $\mathrm{d}I/\mathrm{d}z=0$.

The set of Eqns (2.1.1) is broken up into two independent equations at $K=\mu_K=0$ and $\widetilde{\Theta}_\mathrm{n}=\Theta_{01\mathrm{n}}=0$, which were given in Ref. [15].

2.2 Quasi-stationary case

The approximation $D=\mu=\mu_\mathrm{n}=\mu_K=\mu_3=0$ holds down to ultrashort light pulses ($\tau_\mathrm{p}\sim1-10$ ps) traversing the fibre waveguides [45, 46]. Criterion of its validity will be discussed below.

In the above approximation, Eqn (2.1.1) goes over to the quasi-stationary equations [33, 34] (wherein time τ is present

† A similar switch was put forward simultaneously by Jensen [36] in the particular case of light coupling into one of the identical TCOWs.

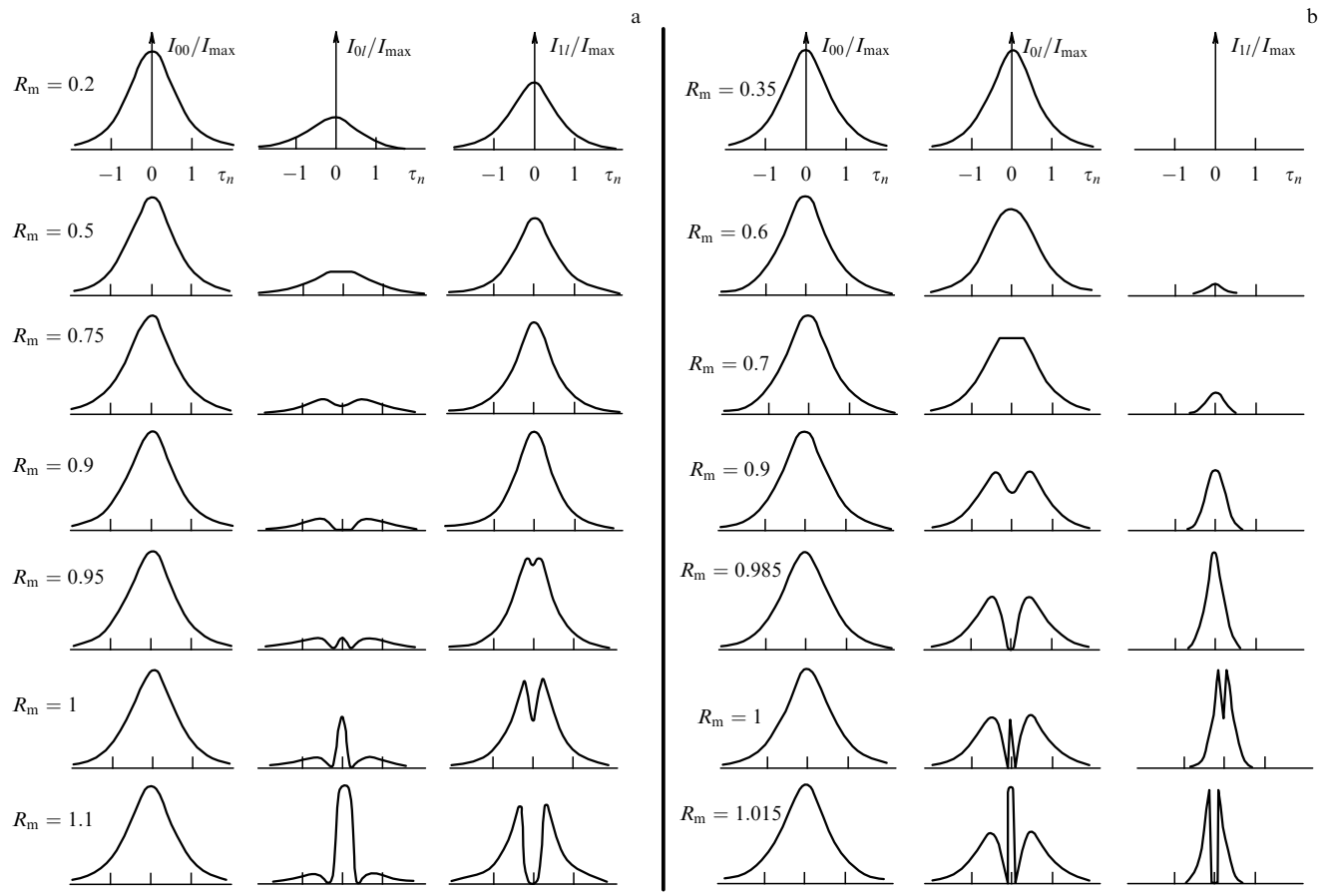

Figure 2. Pulse shapes relating to the zeroth wave $I_{00}/I_{\max} = 1/\cosh(\tau_n)$ at the input, as well as to the zeroth wave $I_{0l}(\tau_n)/I_{\max}$ and first wave $I_{1l}(\tau_n)/I_{\max}$ at the output; $\tau_n \equiv \tau/\tau_p$ is the normalized time in the accompanying frame of reference; $R_m \equiv I_{\max}/I_{0M}$; $R_1 \equiv I_{10}/I_{0M} = 0$, $\alpha = \nu = \widetilde{\Theta} = 0$, $D = 0$, $\mu = \mu_n = \mu_K = \mu_3 = 0$; (a) $L = 1.4\pi$; (b) $L = 2\pi$.

only as a parameter) which were analyzed in Ref. [1]. As this takes place, equations with $\Theta_{01} \neq 0$ reduce to those with $\Theta_{01} = 0$ by the use of a trivial substitution [1, 55]. In this case their solution is expressed in terms of elliptic functions $\mathrm{cn}(L, r)$, $\mathrm{sn}(L, r)$, and $\mathrm{dn}(L, r)$, for which the simple approximations were found over the self-switching region: $r \approx 1$, $\exp L \gg 1$ [1]. To cite an example, for the simplest event of identical ($\alpha = 0$, $\Theta_0 = \Theta_1 = \Theta$, $\nu = 0$) UDCWs and one (zeroth) wave at the system input, the jth-wave intensity at the output is determined by the formula [35, 36]:

$$J_{jl} = \frac{R_0}{2}\left[1 + (-1)^j \,\mathrm{cn}\,(L, r)\right], \tag{2.2.1}$$

where $r = I_{00}/I_{0M} \equiv R_0$, $J_{jl} \equiv I_{jl}/I_{0M}$, $I_{jl} \equiv I_j(z = l)$, $I_{j0} \equiv I_j(z = 0)$, $j = 0, 1$ with $I_{00}(t)$ being the time-dependent function defining the shape of the input pulse.

It follows from (2.2.1) that for the input intensity [35]

$$I_{00} = I_M^{(j)} = I_{0M}\left[1 + (-1)^j 8\exp(-L)\right] \tag{2.2.2}$$

all the output radiation is concentrated either on the zeroth ($j = 0$, $I_{0l} = I_{00}$, M_0 point of the system) or on the first ($j = 1$, $I_{1l} = I_{00}$, M_1 point of the system) wave (see Fig. 1). The differential gain at $I_{00} \approx I_{0M}$ constitutes [35]

$$k \equiv \frac{\partial I_{0l}}{\partial I_{00}} \approx \frac{\exp L}{8}. \tag{2.2.3}$$

Assessment of TCOW in the GaAs crystal at $\lambda = 1.06$ μm places the critical power $I_{0M}S$ at about 14 W with the power gain $\partial I_{0l}/\partial I_{00}$ equal to approximately 500 [35, 1]. Close to the exciton resonance, Θ magnitude is essentially larger, whereas I_{0M} is accordingly smaller. For the dual-core fibre waveguide with $\Theta \sim 10^{-12}$ esu (see, for instance, Ref. [15]) the critical intensity of order 10^9 W cm^{-2} was estimated in Refs [37,1], i.e. the critical power of order 100 W. It should be emphasized that Θ depends not only on the nonlinear properties of the waveguide material but also on the field density in the waveguide determined by the parameter $V = 2\pi a(n_j^2 - \bar{n}^2)^{1/2}/\lambda$, where n_j and $\bar{n}$ are the refractive indices of the light-carrying core of radius a and the cladding, respectively.

Let the bell-shape pulse in the form of a 'zeroth' wave be applied to the system with identical UDCWs:

$$I_{00}(t) = \frac{I_{\max}}{\cosh\left[(t - t_{\max})/\tau_p\right]},$$

where $I_{\max}$ is the maximal intensity of the incident radiation peaked at the point in time $t_{\max}$, which is advisable to be presented in the form $I_{\max} = I_{0M}R_m$ with $I_{10} \equiv I_1(z = 0) = 0$. Here $R_m \equiv I_{\max}/I_{0M}$ defines the ratio between the maximal input intensity and the critical one.

The form of the output pulses is described by the solution to Eqn (2.2.1).

The left pulse in Fig. 2 corresponds to the input pulse and its shape is universally unchanged, whereas the middle and

right pulses apply to those emerging as the zeroth and first waves, respectively. The magnitude of R_m undergoing a rise from the top down is also displayed in the figure.

Figure 2a at $R_m = 0.9$ and Fig. 2b at $R_m = 0.985$ are consistent with $I_{max} = I_M^{(1)}$, whereas Fig. 2a at $R_m = 1.1$ and Fig. 2b at $R_m = 1.015$ correlate with $I_{max} = I_M^{(0)}$.

As seen from Fig. 2, the essential shortening of the pulses as well as rectangular pulse formation and some other intriguing applications of the process in question are made possible. Taking into consideration that the minimal time of radiation self-switching in the system given is restricted by the time of the nonlinearity relaxation which comprises 10^{-14} s in the case of fused quartz, it may be inferred that the pulse length can be shorten down to 10^{-14} s. This conclusion was first confirmed experimentally in Ref. [46] (see Section 3.4). A possibility of pulse shortening by this means was originally revealed in Ref. [74]. It has been proposed to employ the pulse self-switching for restricting their intensities or making the pulse selection by the intensity [35].

2.3 Effect of dispersion and phase self-modulation

To complete the effective self-switching of radiation at low input intensities one may use, as followed from formulas $I_{0M} = 4K/|\Theta|$ and (2.2.3), long systems with UDCWs possessing reasonably large L parameter at small K and, hence, at small I_{0M}. Such systems can be realized around various optic-fibre waveguides: dual-core fibre-optical waveguide (TCOW); birefringent optical waveguide with UDCWs of different polarizations, and, finally, double-mode fibre-optical waveguide with two unidirectional coupled optical modes.

To observe and put to use the effect of radiation self-switching it is worthwhile applying the ultrashort light pulses to the fibre-optical waveguide (see [43] and Section 3.2). However, in the case of lengthy fibre-optical waveguide and ultrashort light pulses the combined influence of second-order dispersion and phase self-modulation may prove to be essential and cannot be neglected.

If $D_n \neq 0$ and $\mu = \mu_n = \mu_K = \mu_3 = \nu = \alpha = 0$, $\Theta_0 = \Theta_1 = \Theta$, then Eqn (2.1.1) goes over to the following equations [43, 47, 105]:

$$2i\frac{\partial A_0}{\partial z_n} + D_n\frac{\partial^2 A_0}{\partial \tau_n^2} = -LA_1 - \Theta_n|A_0|^2A_0\,,$$

$$2i\frac{\partial A_1}{\partial z_n} + D_n\frac{\partial^2 A_1}{\partial \tau_n^2} = -LA_0 - \Theta_n|A_1|^2A_1\,, \qquad (2.3.1)$$

here $\Theta_n = 2\pi l\Theta/\lambda\beta$, which represent the straightforward generalization of the equations [33, 34, 1] to the event of a dispersive medium. The particular case of $D_n = 0$ has been examined elsewhere [1].

Apart from integral (2.1.2), Eqns (2.3.1) have another integral [43, 47]:

$$G = \int_{-\infty}^{\infty}\left[-\frac{1}{2}D_n\left(\left|\frac{\partial A_0}{\partial \tau_n}\right|^2 + \left|\frac{\partial A_1}{\partial \tau_n}\right|^2\right) + L\,\mathrm{Re}\,(A_1A_0^*) + \frac{\Theta_n}{4}\left(|A_0|^4 + |A_1|^4\right)\right]\mathrm{d}\tau_n \qquad (2.3.2)$$

representing generalization of the integral treated in Refs [33, 34, 1] to the event of a dispersive medium.

2.3.1 On the system sensitivity to dispersion in the nonsoliton regime. The process of self-switching as applied to the bell-shape ultrashort pulse was numerically investigated in Ref. [59] with allowance made for the joint influence of dispersion and phase self-modulation (for $\mu = \mu_n = \mu_K = 0$). For definiteness sake, we considered a particular case of the system based on TCOWs. The calculations permitted the following conclusions to be drawn [59]:

(1) The pulse-valley depth in the central part of output pulses becomes incomplete for definite and rather enhanced dispersion $|D_n|$ (see Fig. 2), even though the UDCWs are identical and $I_{max} = I_M^{(j)}$ [see Eqn (2.2.2)].

(2) The larger L, the greater the joint influence of dispersion and phase self-modulation on the radiation self-switching. For example, at $L = 1.4\pi$ the latter phenomenon is impaired with decidedly higher dispersion level as compared to that at $L = 2\pi$.

(3) If $\mathrm{sgn}\,\Theta D = \mathrm{const}$ and $|D_n| = \mathrm{const}$, then the time-dependent profiles of output intensities almost coincide under changes of Θ and D signs.

(4) The joint effect of dispersion and nonlinearity on the output pulse shape depends on the ΘD sign and on that point wherein the system should be placed at $D = 0$. If $D = 0$ conforms to the M_1 point, then at $\Theta D < 0$ (self-stretching of pulses) the joint influence of dispersion and phase self-modulation corrupting the pulse self-switching is much weaker than that at $\Theta D > 0$ (self-compressing of pulses). If $D = 0$ conforms to the M_0 point, then at $\Theta D < 0$ the above effect, on the contrary, is somewhat heightened as compared with the case of $\Theta D > 0$.

As the severity of influence on the part of D_n depends on the L parameter determining the self-switching steepness as well as on the ΘD sign, the conditions allowing the dispersive term to be ignored and the consideration of $D_n = 0$ need not be reduced to familiar conditions for isolated waveguides: $l \ll l_d \approx \tau_p^2/2D$ and $l \ll l_{nl,\tau} \approx \tau_p\sqrt{\lambda/(4\pi|\Theta|I_{00}D)}$. The levels of $|D_n|$ starting from which the D_n influence shows itself have been cited in Ref. [59] for various values of L and $\mathrm{sgn}\,\Theta D$. By way of example, at $L = 2\pi$ and $\Theta D < 0$ the effect of D_n for the M_1 point makes itself evident by starting from $|D_n| \approx 10^{-3}$, whereas at $|D_n| \ll 10^{-3}$ the term involving D_n can be neglected. The above effect may be ignored also in the case of ultrashort pulses ($\tau_p \leqslant 1$ ps) and long fibre-optical waveguides ($l > 1$ m), provided $\lambda \approx 1.3$ μm that corresponds to the point with $D = 0$.

2.3.2 Soliton self-switching. The effect of dispersion is liable not only to deteriorate the pulse self-switching, but it also has the ability to enhance the latter by having done complete. For this purpose, dispersion has to compensate the temporal nonuniformity of the nonlinear phase accumulation so that the pulse acquired the phase profile uniform (or nearly uniform) in time, that is to say became a soliton:

$$A_{00}(t) = \frac{\sqrt{I_{max}}}{\cosh\left[(t - t_{max})/\tau_p\right]}$$

with $I_{max} \approx 2D_n/\Theta_n$, i.e. $\pi|\Theta|I_{max}/\lambda\beta \approx |D|/\tau_p^2$.

A question concerning the feasibility of soliton regime under conditions of self-switching in TCOWs and some peculiarities of this regime was put rather long ago [43, 47]. It has been proposed in Ref. [43] that paired solitons are formed in the system at $l_{nl} \approx l_d$, i.e. two bound solitons one of which travels as a zeroth wave (through the zeroth waveguide,

where TCOWs are involved), and the other does as a first wave (through the first waveguide).

Propagation of solitons in TCOWs and some other systems with UDCWs was numerically investigated in Refs [105–114]. It was suggested in Ref. [105] that a fundamental soliton was supplied to the zeroth-waveguide input and its subsequent behaviour was being studied through numerical solution of Eqn (2.3.1). Redistribution of the soliton energy came about between waveguides, but the solitonic shape of the pulse was conserved in each of the waveguides [105]! In other words, the paired solitons were being formed and transfer of energy between them occurred in accordance with the nonlinear theory [35, 1]. However, regions away from the self-switching operation [i.e. $(I_{\max}/I_{0M})^2 \gg 1$ and $(I_{\max}/I_{0M})^2 \ll 1$] were considered solely in Ref. [105]. The conclusions (as applied to solitons) drawn in Ref. [35] were supported for the cases at hand.

The set of Eqns (2.3.1) (i.e. equations from [43, 47, 105] without appropriate references†) was numerically solved in Ref. [106] for a fundamental soliton coupled into one of the TCOWs with consideration of the immediate self-switching region: $I_{00} \approx I_{0M}$. Based on the computer results, the complete soliton switching without decay and shape distortion [i.e. without 'crater' formation and breaking down into isolated parts as with the quasi-stationary case (see Fig. 2)] was demonstrated [106]. Thus, the complete self-switching of soliton energy proved to be possible! This fact owes to the uniformity of the soliton-phase temporal profile, which is characterized by the equal and solely z-dependent phase at all its points. Hence, the soliton is switched as a single whole. It appears to be wholly at the system output either in the zeroth wave, or in the first wave depending on the maximal value of the intensity.

In the case of the fundamental soliton we are up actually against the temporal analogue of a three-dimensional waveguide; therefore, ignoring the phase modulation and variation of the soliton width we arrive in the first approximation at

$$A_j = \rho_j(z) \exp\left[\mathrm{i}\varphi_j(z)\right] \cosh^{-1}(\tau_n) . \tag{2.3.3}$$

Substituting (2.3.3) in Eqn (2.3.1) gives

$$\begin{aligned}
&\mathrm{i}\rho_0' \cosh^{-1}(\tau_n) - \varphi_0' \rho_0 \cosh^{-1}(\tau_n) \\
&\quad = -D_n \rho_0 \cosh^{-1}(\tau_n)\left[1 - 2\cosh^{-2}(\tau_n)\right] \\
&\quad - L\rho_1 \exp(\mathrm{i}\psi) \cosh^{-1}(\tau_n) - \Theta_n \rho_0^3 \cosh^{-3}(\tau_n) , \\
&\mathrm{i}\rho_1' \cosh^{-1}(\tau_n) - \varphi_1' \rho_1 \cosh^{-1}(\tau_n) \\
&\quad = -D_n \rho_1 \cosh^{-1}(\tau_n)\left[1 - 2\cosh^{-2}(\tau_n)\right] \\
&\quad - L\rho_0 \exp(-\mathrm{i}\psi) \cosh^{-1}(\tau_n) - \Theta_n \rho_1^3 \cosh^{-3}(\tau_n)
\end{aligned} \tag{2.3.4}$$

where the prime denotes differentiation with respect to $z_n/2$. In so doing the temporal profile of the field $\cosh^{-1}(\tau_n)$ may be described and estimated in the same manner as the spatial field profile was taken into consideration in deriving the equations in Refs [33, 34, 43] and Eqn (2.1.1) (see also Ref. [1]), namely, multiply both the sides of Eqn (2.3.4) by $\cosh^{-1}(\tau_n)$ and thereafter integrate them with respect to τ_n between $-\infty$ and ∞. It follows then

$$\begin{aligned}
&\mathrm{i}\rho_0' = -L\rho_1 \sin\psi , \\
&-\varphi_0'\rho_0 = \frac{D_n\rho_0}{3} - L\rho_1 \cos\psi - \frac{2}{3}\Theta_n\rho_0^3 , \\
&\mathrm{i}\rho_1' = L\rho_0 \sin\psi , \\
&-\varphi_1'\rho_1 = \frac{D_n\rho_1}{3} - L\rho_0 \cos\psi - \frac{2}{3}\Theta_n\rho_1^3 ,
\end{aligned} \tag{2.3.5}$$

that is equivalent to the system of equations

$$\begin{aligned}
&\psi' = \frac{L(I_0 - I_1)}{\sqrt{I_0 I_1}} \cos\psi + \frac{2}{3}\Theta_n(I_1 - I_0) , \\
&I_0' = -2L\sqrt{I_0 I_1} \sin\psi , \qquad I_1' = 2L\sqrt{I_0 I_1} \sin\psi .
\end{aligned} \tag{2.3.6}$$

Hence, we arrived at the set of equations identical to that for the quasi-stationary case [35, 1] and which involves an effective nonlinear coefficient equal to $(2/3)\Theta$ rather than Θ. The critical intensity increases, accordingly, by half again the value for the quasi-stationary case and this conclusion approximately conforms with numerical findings in Refs [106, 108].

Thus we can adopt the theory developed in Ref. [1] when describing the phenomenon of fundamental soliton self-switching in the first approximation and in so doing we interpret the $\varphi_j(z)$ phases as the soliton phase in the jth wave (in the jth waveguide, if TCOWs are dealt with), whereas $I_j(z)$ may be regarded as the soliton peak intensity. In evaluating numerical parameters for the nonlinear coefficient use could be made of the following coefficient

$$\Theta_{\text{eff}} \simeq \frac{\int_{-\infty}^{\infty} \Theta \cosh^{-4}(\tau_n)\, \mathrm{d}\tau_n}{\int_{-\infty}^{\infty} \cosh^{-2}(\tau_n)\, \mathrm{d}\tau_n} = \frac{2}{3}\Theta , \tag{2.3.7}$$

resulted from averaging over the temporal profile (akin to averaging over the transverse cross section in deducing the equations in Refs [33, 34] (see also Section 2 in Ref. [1]). Under this rough estimation, the temporal profile is assumed to be constant and proportional to $\cosh^{-1}(\tau_n)$ in the first approximation although its slight variation during the progress of the switching just takes place [106]. This fact apparently lies at the basis of explanation for some quantitative discrepancy between the above estimate of the critical intensity and the numerical results [106].

More complicated form of the probe function was invoked in Ref. [112]:

$$A_j = \rho_j(z) \exp\left[\mathrm{i}\varphi_j(z) + \mathrm{i}b(z)\tau^2\right] \cosh^{-1}\left[\frac{\tau}{\tau_p(z)}\right]$$

and a set of ordinary differential equations was developed for $\rho_j(z)$, $\varphi_j(z)$, $\tau_p(z)$, and $b(z)$. These equations elude analytical solving in the region wherein $l_d \simeq l_c$. But just this region is of prime interest for us, because it conforms to the self-switching event ($|\Theta|I_{\max} \simeq 4K$) and soliton formation ($\pi|\Theta|I_{\max}/\lambda\beta \simeq |D|/\tau_p^2$) at one time.

Study on the soliton switching by application of a weak alternating signal was conducted in Ref. [110] using a numerical approach. In doing so, the figure from Ref. [110] essentially coincides with Fig. 6 appeared below and displayed earlier in Ref. [43], i.e. it illustrates the principle of operation of a discrete optical transistor [43] in the 'key' mode

† This is by no means the unique event of improper borrowing; for instance, equations from Refs [33, 34] were used in Ref. [81] without any literature citation.

for a concrete form of the envelope ($\operatorname{sech}\tau_n$) for ultrashort pump pulses. Dependence of the soliton-energy transmission coefficient on the input-signal phase [110] is coincident with the analogous dependence in the quasi-stationary state [1, 37].

It should be emphasized that the switching method [33, 37, 43] has been actually discussed in Ref. [110] without proper citation.

The time history of relative maximum positions for two accompanying solitons was studied in Refs [107, 108]. The situation was comprehended when solitons with closely related intensities were fed to the TCOW inputs. If the soliton maxima at the waveguide input are slightly shifted in time with reference to each other, then they shift all the more during the propagation, i.e. as though one soliton begins to be ahead of the other, whereas this latter lags behind. The process at hand is enhanced multiply if the soliton self-frequency shift takes place, being governed by the Raman effect [114] (and defined by the term including μ).

It is common knowledge that the waves polarized along and orthogonally to the optical axis travel at different velocities in the birefringent medium. However, the availability of nonlinearity (the 'cross' coefficient Θ_{01}) at fairly high input amplitudes stabilizes the waves against their 'walk-off' (splitting) which is due to the birefringence effect [115]. In other words, there occurs a mutual 'trap' of normally polarized solitons travelling with equal velocities ('fast' polarization is retarded, and 'slow' one accelerates). It was suggested to devise the logic elements by applying the principle of the soliton stabilization [116]: according to whether the signal pulse is fed or not, the soliton of polarization orthogonal to this pulse is either trapped and retarded or not and, correspondingly, it either appears or not in the 'clock window'. The frequencies of mutually trapped solitons are slightly shifted (by the value of order 0.5 THz) in opposition. Notice that the terms involving K and $\widetilde{\Theta}$ which are responsible for the UDCW self-switching have been neglected in Refs [115, 116].

2.4 Influence of nonlinearity relaxation inertia, nonlinear dispersion of group velocity, and the coupling coefficient dispersion

The factors discussed which are allowed, correspondingly, for the terms in Eqn (2.1.1) with coefficients μ, μ_n, and μ_K, have been studied (at $D = 0$) in Ref. [69]. Their action is manifested, among other factors, in the symmetry breaking for the pulses at the output (Fig. 3). The reason is that the leading and trailing edges of the pulse are to be found in different conditions. By this means, where influence of the parameter μ is concerned, i.e. nonstationarity of the nonlinear response, we can say that the cubic nonlinearity has yet no time to take the steady value Θ on the pulse leading edge and proves to be smaller than this value, i.e. as if the critical intensity on the pulse leading edge is extended as against I_{0M} and the system has not yet 'reached' the point of self-switching.

The term with μ_K accounts for dispersion of the coupling coefficient. The physical reason for this looks as follows. Short pulses possess a wide frequency spectrum. Different coupling coefficients correlate with various frequency components, i.e. a spread of coupling coefficient magnitudes within the pulse arises. This spread shows up most vividly for TCOWs as their coupling coefficient strongly depends on frequency. For other UDCWs the spread is essentially smaller. Lest the operation of a self-switch be disrupted, the relative spread of coupling coefficient values is bound to be much smaller than k^{-1}, where k is the gain estimated by Eqn (2.2.3) in the simplest event.

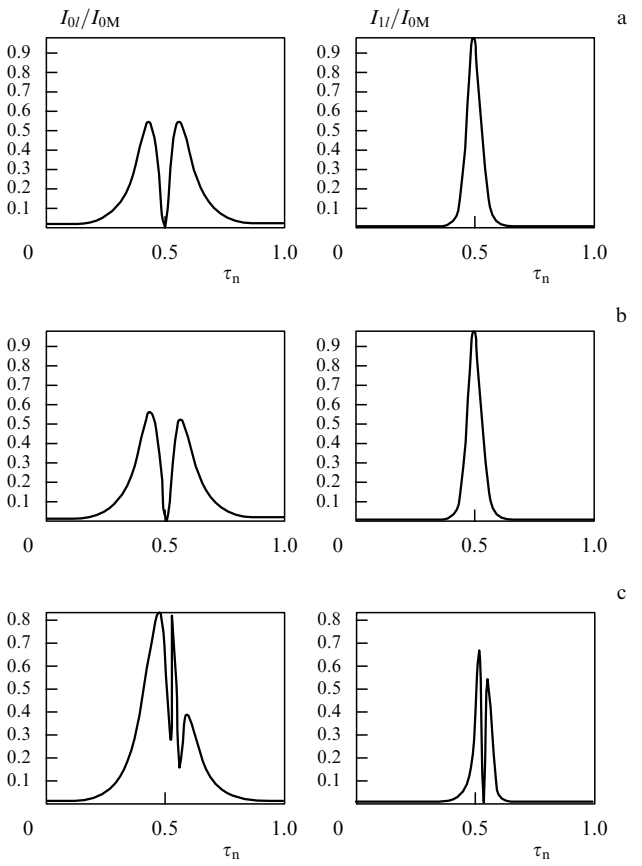

Figure 3. Shape of the output pulses in the zeroth $I_{0l}(\tau_n)/I_{0M}$ and first $I_{1l}(\tau_n)/I_{0M}$ waves, where $\tau_n \equiv \tau/\tau_p$ is the normalized time in the accompanying reference system: (a) $\mu = 0$; (b) 10^{-3}; (c) 10^{-2}; $\mu_n = 0$, $\mu_K = 0$, $L = 2\pi$, $\alpha = D = \nu = \mu_3 = 0$, $\Theta_j = \Theta$, $\Theta_{01} = \widetilde{\Theta} = 0$ (taken from Ref. [69]).

Let us render concrete an appraisal of

$$\mu_K \simeq K^{-1}\tau_p^{-1}\frac{\partial K}{\partial\lambda}\frac{\partial\lambda}{\partial\omega} + \frac{T_0}{\tau_p\pi}$$

for TCOWs by expressing μ_K in terms of the T_0/τ_p ratio. Numerical estimates show that the value $\lambda(K^{-1}\,\partial K/\partial\lambda) \approx 7$ is typical for TCOWs (possible though are just as slightly lesser, so superior values). Considering that $\tau_p^{-1}(\partial\lambda/\partial\omega) = -\lambda T_0/(2\pi\tau_p)$, the above parameter can be crudely estimated as $|\mu_K| \simeq T_0/\tau_p$.

Computations done in Ref. [69] evidenced that influence of $|\mu_n|$ and $|\mu_K|$ coefficients shows up equally: calculated results agree for $\mu_n = -\mu_K$.

The concurrent effect of terms with μ, μ_n, and μ_K coefficients appears in a number of cases to be tangibly weaker than that of individual terms, i.e. as if they compensate each other [69].

The influence of μ_n and μ_K parameters reveals itself also in strengthening the instantaneous peak intensity of the pulse 'spike' at the first waveguide output (for the first wave) on account of spike sharpening, i.e. its 'compressing' in time [69].

Calculated results also permit estimation of μ, μ_n, and μ_K values beginning with which the pulse self-switching is disturbed [69]. These values were found to be of order 10^{-3} at $L = 2\pi$, and they are substantially higher (of order 10^{-2}) for $L = 1.4\pi$. Thus, if $L \leqslant 1.4\pi$ and there occurs that

$\mu, \mu_n, \mu_K \ll 10^{-2}$, then terms with μ, μ_n, and μ_K in Eqn (2.1.1) are disregarded.

The above findings are useful in forecasting the operation of discrete optical transistors [43] and logic elements [37] based on TCOWs and other UDCWs, wherein the continuous sequence of ultrashort pulses is utilized as a pump (with the aim of estimating the pump and TCOW parameters at which the distortion of output pulses has yet to be neglected).

We shall now give two specific examples with estimates of the coefficients μ, μ_n, and μ_K.

Example 1. Let us assume that a dual-core fibre waveguide made of fused quartz is employed and it is characterized by $T_{nl} \leqslant 10^{-14}$ s, $\Theta \sim 10^{-12}$ esu and the critical intensity of order 10^9 W cm^{-2} for $K \sim 10^{-6}$ [37, 40, 45], conforming to the power around 100 W with a cross-sectional area S of about 10^{-7} cm^2. To one of TCOWs let there fed ultrashort light pulses with $\lambda \approx 1.3$ μm, i.e. $T_0 = \lambda/c \approx 4.3 \times 10^{-15}$ s, whose amplitude corresponds to the intensity $I_M^{(1)}$. Then $\mu \leqslant 10^{-2} \times \tau_p$, $\mu_n \simeq 1.4 \times 10^{-3}\tau_p$, $\mu_K \simeq -4 \times 10^{-3}\tau_p$, where the pulse duration τ_p is measured in ps. In compliance with above results for pulses of duration under 1 ps, the effect of terms with μ, μ_n, and μ_K coefficients may be essential already at $L \geqslant 1.4\pi$ ($l \geqslant 4.2$ m). For pulses of duration above 10 ps, the effect of these terms are disregarded even at $L \approx 2\pi$ ($l \approx 6$ m). By way of example, terms involving μ, μ_n, and μ_K coefficients in Eqn (2.1.1) can be neglected with confidence under experimental conditions ($\tau_p \geqslant 20$ ps) [45, 46], the more so as radiation was shifted experimentally in wavelength to shorter range: $\lambda = 0.53$ μm, i.e. $T_0 = 1.7 \times 10^{-15}$ s.

Example 2. Let us next assume that TCOWs are fabricated from a layered structure of the GaAs(100 A)/$Al_{0.3}Ga_{0.7}As$(100 A) ($n \approx 3.5$) type, which represents a multi-quantum-well structure with a nonlinear coefficient $\Theta \sim 10^{-4}$ esu. Provided $K \approx 2 \times 10^{-4}$, the critical intensity comprises 1.3×10^4 W cm^{-2} resulting in a power some 1.3 mW for $S \sim 10^{-7}$ cm^2. The time of the nonlinearity relaxation diminishes down to $T_{nl} \approx 0.04$ ns on bombarding this structure with protons [97]. Let light pulses of $\lambda \approx 0.9$ μm ($T_0 = 3 \times 10^{-15}$ s) and duration $\tau_p \approx 40$ ns be coupled into one of the TCOWs. Then the term with $\mu \sim 10^{-3}$ may show itself, if the distance of two linear light transfer from one core to the other confines itself to the TCOW length ($L = 2\pi$, $l = 3$ mm) and the effect of terms with μ_n and μ_K is overlooked. For shorter pulses of $\tau_p \approx 4$ ns, the term with $\mu \sim 10^{-2}$ will be exhibited already at $L = 1.4\pi$ ($l \approx 2$ mm).

In the event of soliton self-switching, the inclusion of terms with μ, μ_n, and μ_3 leads to enhancement of the critical intensity [109].

2.5 On the speed of self-switches response

The speed of the self-switch response may be limited by factors being allowed for the μ, D, μ_K, and μ_n coefficients in Eqn (2.1.1), for instance, through the second-order dispersion. But the main limitation usually concerns the nonlinearity inertial effect and therefore for simplicity we assume that $D = \mu_K = \mu_n = \mu_3 = \nu = 0$. It should be emphasized that in this situation the speed of response characterizing the switches and optical transistors at hand is determined only by the time of relaxation of the medium optical nonlinearity rather than the time of light travelling along the waveguides. To have a 'feeling' for this conclusion, imagine the sequence of the zeroth-wave square pulses alternating in intensity, with values given by Eqn (2.1.3) with $j = 0$ and $j = 1$, and coupling into the system input. As this takes place the length of pulses and interval between them fall far short of the time of light transit along the waveguides, and yet they are well over the time of nonlinearity relaxation. If the switching time was determined by the time of light travelling along the waveguides, then the system would have not obviously managed to switch the pulses. But a switching event proceeds. The matter is that in this case one may ignore the term accounting for nonlinearity relaxation in nonstationary equations (2.1.1) which govern such switching. In which event nonstationary equations (2.1.1) become quasi-stationary [33, 34, 1], wherein the running time $\tau = t - z/u$ is present as a parameter. Analysis of equations unambiguously showed that these pulses would be switched [33, 34, 1]: one pulse would be found in the zeroth wave at the system output, the next — in the first wave, etc. The experiment favoured the above conclusions [46] (see also Section 3.4) and demonstrated the valley and spike on the output ultrashort pulse of duration under 5 ps, whereas the time of light pulse travelling comprised 5 ns, i.e. it was as great as 1000-fold.

3. Experimental evidence of the UDCW nonlinear power transfer and self-switching

This section is concerned with the experiments the aim of which is to disclose the phenomenon of light self-switching predicted in Refs [33 – 36]. Attention was drawn as far back as in 1984 [37] to the fact that observation of this phenomenon in fibre-optical waveguides hold much promise, and just in these waveguides it has been first observed. In the experiments [40, 45, 46], laser radiation with a single transverse mode was coupled into one of the cores possessed by a dual-core fibre waveguide and the distribution of power between cores at the system output was investigated as a function of input intensity. Cores together with a common cladding made from fused quartz have formed the single-mode waveguides tunnel-coupled with each other. The gap d between cores was small ($d \approx 8$ μm), which is why the controllable coupling of laser radiation into one of the cores (without affecting the other) has always posed a problem. To solve the latter, a special procedure of radiation coupling was developed [40, 117] whose essence consists in the following (see Fig. 4). Radiation ($\lambda = 0.53$ μm) was transmitted through the glass wedge *1* and then was focused on the end of the waveguide *3* with the aid of a micro objective *2*. The focused radiation reflected partially from the waveguide end, then it was transmitted again through the

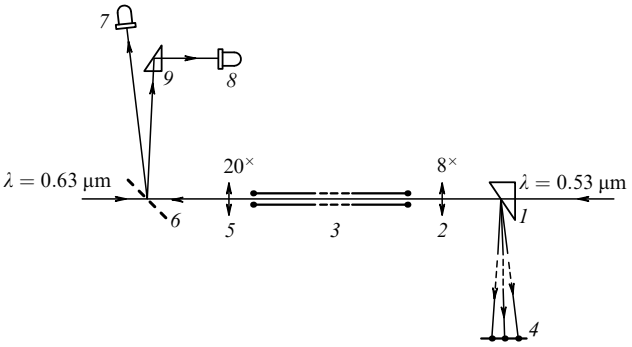

Figure 4. Layout of the first experiment on light nonlinear pumping over in TCOWs: *1* — glass wedge; *2* — 8× micro objective; *3* — waveguide; *4* — screen; *5* — 20× micro objective; *6* — removable mirror; *7, 8* — photocathodes; *9* — prism.

micro objective *2* and reflected from the wedge-*1* surface, and, finally, this radiation was incident on the screen *4*. Synchronous with propagation of the above laser beam, 'auxiliary' radiation of an He–Ne laser ($\lambda = 0.63$ μm) was coupled into the waveguide from its opposite side by the use of a micro objective *5*. This radiation fell on the screen *4* after being transmitted through the waveguide *3* and micro objective *2* as well as reflected from the wedge *1*. Therefore, the images of waveguide-core input faces and focal spot of coupled radiation were viewed on the screen. The image of the input face for one of the waveguide cores and that of the focal spot were brought into coincidence by moving the waveguide input face with the help of micrometric screws and in doing so the coincidence between longitudinal axes of the coupled light beam and the light waveguide core could be gained.

3.1 Nonlinear transfer of light energy in TCOWs

Under first experimentation [40], the second-harmonic pulse ($\tau_p \approx 80$ ns) from the neodymium-glass laser in the Q-switching mode was applied to one of the waveguide cores. In this experiment (see Fig. 4), the nonlinear transfer of radiation power in TCOWs has been observed for the first time and the results corresponded closely to theory (Fig. 5), i.e. the feasibility of radiation self-switching was indirectly confirmed. However, the direct observation of the phenomenon itself has not met with success mainly due to parasitic stimulated Brillouin scattering (SBS) and TCOWs of insufficiently good quality.

The experiment conducted in Ref. [40] can be viewed also as an approach to measuring the coupling coefficient K and nonlinear coefficient Θ of optical waveguides. The theoretical curve in Fig. 5 fitting experimental data was calculated according to Eqn (2.2.1) for $L = 0.24\pi$ and $P_{0M} = 95$ W. From $L = 0.24\pi$ at $l = 18$ cm it follows that $K \approx 5.2 \times 10^{-7}$. Given K and P_{0M}, we arrive at $\Theta \approx 2Kc\beta S/\pi P_{0M} \approx 4 \times 10^{-13}$ esu. For the coefficient n_2 appearing in the known expression [7, 12, 15] $n = n_0 + n_2\langle E^2\rangle$, the following estimate $n_2 \approx \Theta/2n_0 \approx 1.3 \times 10^{-13}$ esu was made, which is in agreement with tabulated data (see, for instance, [15]).

Shortly after publishing the paper [40], nonlinear transfer of radiation energy was observed in the analogous experiment [76], in which TCOWs were fabricated around layered periodic structure of the multiquantum-well (MQW) type: GaAs(100 A)/$Al_{0.3}Ga_{0.7}As$(300 A) involving 25 periods. In doing so the critical power was reduced down to about 1 mW because of resonance enhancement of cubic nonlinearity in the vicinity of exciton resonance†, tuning out from which comprised $\Delta E = 56$ meV. Furthermore, $n_2 \sim 10^{-7}$ cm^2 W^{-1}, loss coefficient approximately equals 6.5 dB mm^{-1} ($\delta \approx 15$ cm^{-1}), and, finally, TCOW length $l \approx 2$ mm. GaAlAs laser diode at room temperature served as a radiation source ($\lambda = 0.85$ μm and $\tau_p \approx 100$ ns), whereas TCOWs were cooled down to a temperature of 180 K, exciton resonance whereat corresponded to $\lambda = 0.82$ μm. Unfortunately, the procedure of radiation injection into a waveguide has not been described in Ref. [76]. Two more years later the nonlinear radiation transfer was observed in the ridge TCOWs based on MQW $Ga_{0.7}In_{0.3}As$(150 A)/GaAs(150 A) structures for the wavelength $\lambda = 1.15$ μm [87]. Tuning out from the exciton resonance measured $\Delta E = 40$ meV with $n_2 = 2.25 \times 10^{-7}$ cm^2 W^{-1}, loss coefficient $\delta = 30$ cm^{-1}, and the length of a single linear energy transfer comprising about 0.4 mm. Longitudinal distribution of radiation energy over waveguide axis has been studied by a procedure of its sequentional cleaving off.

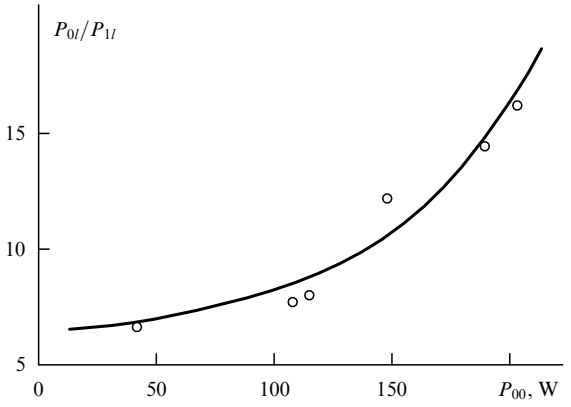

Figure 5. Power ratio at the TCOW output (waveguide length $l = 18$ cm) as a function of radiation power at the input (light is coupled into one of the waveguides): open circles — experimental data [40], solid line — calculated by (2.2.1).

3.2 On a possibility of observation and use of the radiation self-switching effect; a discrete optical transistor

In order to observe the phenomenon considered it was suggested [43] to feed the train of ultrashort light pulses into one of the waveguide cores, because in this case the parasitic influence of stimulated Brillouin scattering is eliminated and the threshold intensity of a waveguide-end breakdown increases. The discrete analogue of an optical transistor has been also proposed [43] with a continuous sequence of ultrashort pulses of intensity close to a critical one (see Fig. 6) being used as a pumping source. In the absence of light dispersion, the right-angled shape of ultrashort pumping pulse looks as optimal, and yet if dispersion is essential then solitonic form is preferable: $\cosh^{-1}(\tau_n)$ (see Section 2.3). In these events, complete switching of pulses is possible.

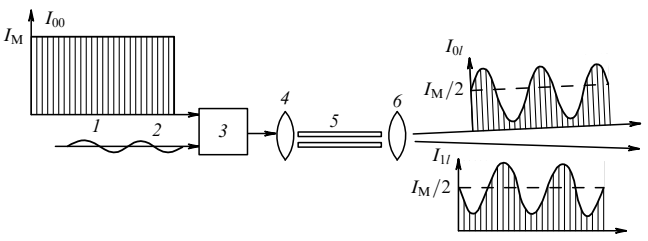

Figure 6. Schematic diagram of a TCOW-based discrete optical transistor: *1* — pumping pulses; *2* — signal; *3* — mixer; *4* — entrance micro objective; *5* — TCOW; *6* — dividing micro objective (taken from Ref. [43]).

3.3 Observation of light self-switching in TCOWs and demonstration of possibilities for optical transistor development

Advanced dual-core optic-fibre waveguide, as compared with that employed in Ref. [40], was used in further experiments [45] two years later. The former was fabricated on the base of fused quartz and had two parallel equal cores of $a \approx 1.3$ μm radius in the common cladding with difference in refraction

† Attention was drawn to this fact still in Ref. [35].

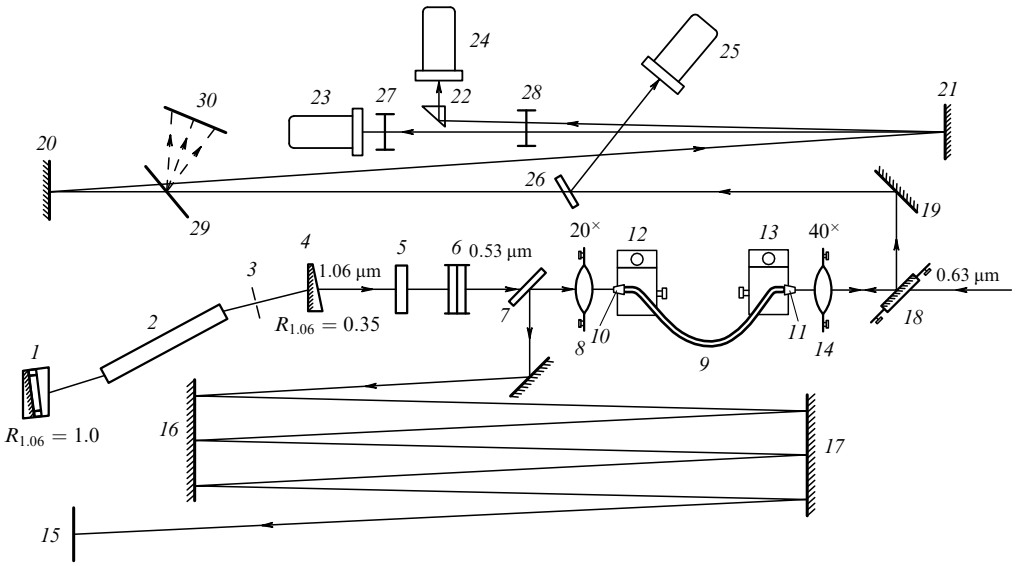

Figure 7. Layout of the first experiment on light self-switching in TCOWs [45]: *1–4* — laser with passive mode synchronization; *5* — frequency doubler; *6* — filter; *7* — mirror; *8* — micro objective; *9* — double-core optic-fibre waveguide; *10, 11* — holders; *12, 13* — micrometric adjusting gears; *14* — micro objective; *15* — screen; *16–21* — mirrors; *22* — prism; *23–25* — optical receivers; *26* — glass plate; *27, 28* — filters; *29, 30* — removable diffraction grating and screen (for revealing the stimulated Raman scattering).

indices of the core and cladding reaching $\Delta n \approx 0.005$ and $d \approx 8.6$ μm. In this experiment (the scheme whereof is displayed in Fig. 7) a train of ultrashort light pulses pertaining to the second harmonic of an Nd : YAG laser ($\lambda = 0.53$ μm) operated in the regime of passive mode synchronization, was coupled into one of the waveguide cores by employing the refined technique [117]. Light beams emerging from both the cores were spatially separated and each of them was set off to its own photocathode (*23* and *24* in Fig. 7). Approximately 8%-fraction of the coupled radiation power was directed to the third photocathode *25* (of sensitivity ≈ 1.15 mA W^{-1}) with the aid of plate *26*. Owing to small losses in the optical waveguide we may consider that $I_{0l} + I_{1l} = I_{00}$. Electric signals from photocathodes with various time delays were applied to the same input of an 'Tektronix' oscillograph ($\Delta f \sim 1$ GHz, $r_{in} = 50$ Ohm) on whose screen we could distinguish three trains of ultrashort pulses (see Figs 8–11): the first train (the very left) is the signal proportional to the input one; the second and third trains match the output signals from one and the other cores.

By selecting the light filters in holder *27*, an equality between amplitudes of the second and third pulse trains on the screen at $I_{0l} = I_{1l}$ was reached. Due to broadening of the third-train pulses (after travelling through a delay cable 50 m in length) the latter merged together in the lower part of the screen.

The apparatus employed has enabled one to monitor the radiation power averaged over the time interval $\tau_a \approx 0.5$ ns. Doing so led to underestimating the maximum intensity of separate train pulses ($\tau_p \approx 50$ ps) and their envelopes on the oscillograph screen approximately by an order of magnitude. Taking into consideration above data, the appraised coefficient of conversion from the amplitude of 'input' signal on the oscillograph screen to the power comprised some $(0.08 \times 50\ \text{Ohm}) \times (1.15\ \text{mA W}^{-1}) \times (\tau_p/\tau_a) \approx 0.46\ \text{mV W}^{-1}$.

Power variation for pulses within each train provided a way for keeping track of the power distribution for each separate pulse over TCOW outputs in relation to its input intensity. To put it differently, owing to bell-shape change of separate pulse intensity (from pulse to pulse) within a train we arrived at a kind of input pulse 'sweeping' into an intensity sequence from the zero point to the envelope maximum. Power of the input train as a whole was varied either through the use of light filters *6* or at the expense of the natural scatter in the amplitudes of an envelope for laser pulse trains.

Some refinements were introduced into the experiment discussed [45] by comparison with that in Ref. [40]. Firstly, a 30–40%-reflectance mirror *7* was employed in the optical 'sighting' system that was responsible for branching off the red and green portions of visible light in the screen direction, being larger than those in Ref. [40] by 6–10 times. This served to enhance the image brightness on screen *15* for the input waveguide face, and in turn permitted employment of wide (20×20 cm^2) metallic mirrors *16, 17* placed 170 cm apart in order for increasing the optical path between the entrance objective and the screen up to 10 m and for securing therewith the compactness of all the measuring unit. Secondly, mirror *18* (which replaced the removable mirror *6* from Ref. [40]) reflected more than 95% of a green light emerging from the optical waveguide, and transmitted in excess of 75% of a red light incident on it from the other side. Doing so allowed viewing of enlarged (×2000) image of the entrance waveguide face on screen *15* at all times (controlling the $\lambda = 0.53$ μm-radiation coupling into one of the cores) and simultaneously analyzing of the light pulses emerged from a waveguide exit, on the oscillograph screen. The Nd : YAG laser could operate either in the regime of solitary pulse trains or with repetition frequency of 3 Hz with a consequent lightening of the radiation injection control and unit adjustment.

All optical scheme of the experiment (see Fig. 7), including both the lasers, has been rigidly 'bound' to the massive platform (lying on the air-cushion) of a holographic table. By this means the system was excluded from outer sources of mechanical vibrations. Accuracy of the micrometric displacement of an entrance waveguide face in the direction normal to the light beam was over 0.2 μm per point.

More than one sets of experiments have been conducted. Waveguide characteristics were unvaried in the course of each

run, i.e. $L = \text{const}$. By way of illustration let us consider oscillograms pertaining to four sets of measurements for the waveguide sections with $l = 128$ cm (Fig. 8 — A run), 101 cm (Fig. 9 — B run), 113 cm (Fig. 10 — C run), and 128 cm (Fig. 11 — D run); the input intensity increases from the top down similar to that in Fig. 2 (theoretical estimate of pulse shapes).

A qualitative agreement between experimental (see Figs 8–11) and calculated (see Fig. 2) results was evidenced in these studies.

Experiments permitted a common regularity to be revealed: at small intensities of the coupled radiation ($\leqslant 0.3$ GW cm^{-2}), the shape of envelopes for the second and third pulse trains on the oscillograph screen was unchanged along with a relationship between their amplitudes (Figs 8–11). Such conditions correlate with a linear regime. The area in Fig. 1 where $(I_{00}/I_{0M})^2 \ll 1$ and the curve $T_0(I_{00}/I_{0M})$ is nearly parallel to the abscissa axis, conforms to the latter.

With increase in I_{00} amplitude (i.e. height of the first pulse train), the amplitude of a second (and for the D run — third) train slightly rose but this enhancement was retarded gradually and came to naught. Close to a certain (for a given run) magnitude of the I_{00} amplitude, there occurred a dip at the centre of a second pulse train (Figs 8b, 9b, 10b, and 11d), i.e. a decrease in amplitudes of the train pulses. At the centre of a second pulse train in Fig. 11 and that of a third train in Figs 8–10, the intensity spike was observed in the process. Such situation fits a 'crevasse' in the self-switching curve (see Fig. 1) and a relationship $I_{00} \approx I_M^{(1)}$ linking the amplitudes.

The pulse spike appeared at the centre of a second pulse train (for the D run — at the centre of a third train) with further increase in I_{00} amplitude, whereas a dip was observed (see Figs 8c, 9c, 10d,e, 11e,f) at the centre of a third pulse train (for the D run — at the centre of a second train).

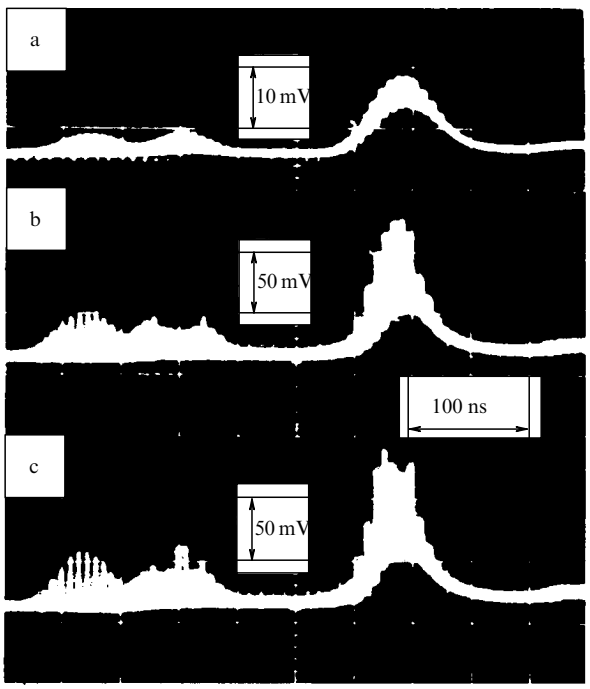

Figure 8. Oscillograms of pulses pertaining to the input signal I_{00} (left pulse train) and output signals I_{0l} (middle train) as well as I_{1l} (right train) [45]. Experimental set is labelled as A.

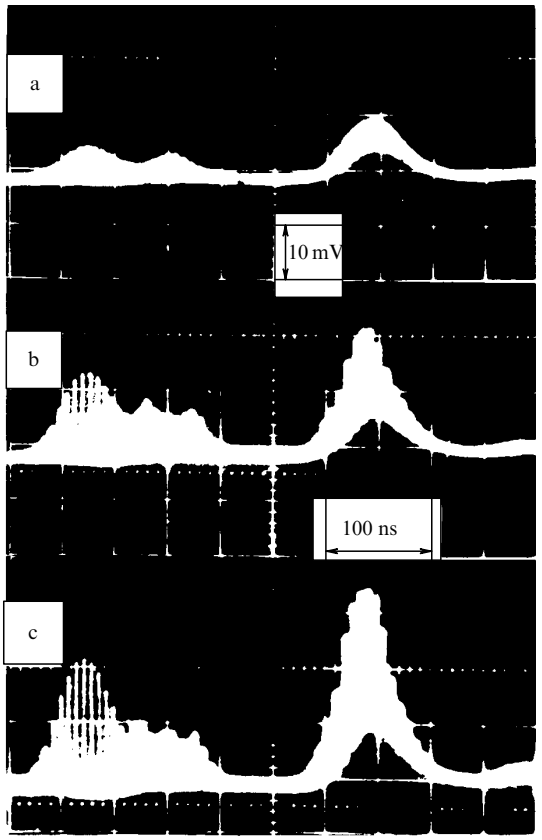

Figure 9. Pulse oscillograms measured in the course of the experimental set B.

The self-switching effect itself can be seen in Fig. 10c–e: the pulse spike at the centre of a second pulse train becomes so pronounced with a small rise in I_{00} amplitude that the second pulse train is again rendered higher than the third one. In this case small differences of the input power are amplified multiply at the system output. Such amplification of the I_{00} differences comes into existence close to the value $I_{00} = I_{0M}$ with $c\beta I_{0M}/2\pi \sim 1$ GW cm^{-2}, which correlates with an estimate of the critical intensity presented in Ref. [37]. For other sets of experiments there occurs $c\beta I_{0M}/2\pi \sim 1$ GW cm^{-2}, too.

The gain $k = \partial I_{0l}/\partial I_{00}$ may be evaluated either from a correlation of Fig. 10 with Fig. 10e (small rise in height of the first pulse train approximately by 20% brings about significantly larger increase in height of the second train around 100%) or from viewing in detail the isolated graphic presentation in Fig. 10e. Let us estimate the gain with the photograph in Fig. 10e. The height difference for adjacent pulses (marked with arrows) from a second train is 5–7 times greater than that for the same pulses in a first train. Considering a modest distinction between the height differences for adjacent pulses pertaining to the first and second trains in the linear regime (in the second pulse train displayed in Fig. 10a this difference is 1.5 times as great as in the first one) we shall arrive at a rough estimation of the optical transistor differential gain: $k \approx 3-5$.

It should be emphasized that the oscillogram in Fig. 10e was recorded under conditions when the amplitude $I_{00} \approx I_M^{(0)} > I_{0M}$, since, firstly, the heights of the most peaked pulses in the second train are brought again into proximity,

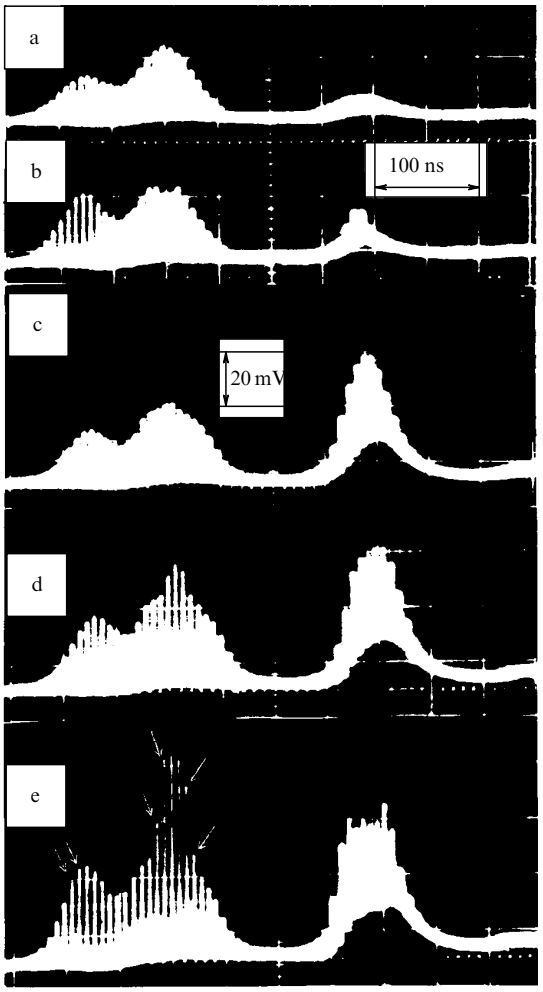

Figure 10. Pulse oscillograms measured in the course of the experimental set C.

and, secondly, the second train height newly becomes greater than that for the third train, i.e. $I_{0l} > I_{1l}$.

In the case of experimental sets A, B (Figs 8, 9), the amplitude I_{00} does not reach the I_{0M} values typical of these sets.

Self-switching effect may be observed also in the oscillograms of the D set (see Fig. 11) where as contrasted to the previous experimental sets the third pulse train (the very right) emerges from the zeroth waveguide, and the second train — from the first waveguide. The amplitude of a second train in Fig. 11b,c is under the amplitude of a third train, while at a greater input intensity (Fig. 11d – f) the amplitude of a second train is already above the third-train amplitude. Figure 11d corresponds to the amplitude $I_{00} \approx I_M^{(1)}$. Evolution of the self-switching event is clearly defined in Fig. 11d – f: with a small rise in input intensity, the pulses from a zeroth optical waveguide (at the centre of a third pulse train) are impetuously built up. As this takes place it is clearly seen in Fig. 11f (complying with the portion of the characteristic nearby the self-switching point M) that the power change at the waveguide output multiply stands out above variation of the input power: second and third pulse trains in a literal sense 'go to pieces' of isolated ultrashort pulses.

It should be emphasized that the shape of the 'total' pulse train (the very left on the oscillograph screen) always remains to be unvaried — bell-shaped — and coinciding with the shape of the initial laser train, i.e. light power is only redistributed between TCOWs.

Correlating Figs 1, 2 with Figs 8 – 11 and determining the amplitude of which pulse firstly recovers from its growth as the amplitude I_{00} goes higher as well as finding the relationship between amplitudes of the second and third trains in a linear regime (by counting the height of the third-train pulses from the 'pedestal') we may conclude that: the second train emerges from the zeroth waveguide in the case of oscillograms presented in Figs 8 – 10, whereas for Fig. 11 — from the first waveguide; inequality $L > \pi$ is obeyed for all the oscillograms with $L \approx 1.8\pi$ for Fig. 10 and $L \approx 1.6\pi$ for Fig. 11.

Whilst the experimental and theoretical results qualitatively coincide, there appears quantitative disparity between them as far as the estimate of a self-switching slope (optical transistor gain) at $I_{00} \approx I_{0M}$ is concerned. First, based on the above-mentioned magnitude of the L parameter, the gain in the event of Fig. 10 according to the theoretical consideration by Eqn (2.2.3) proves to be equal to $\exp(L)/8 \approx 35-50$, i.e. it is about an order of magnitude greater than the measured quantity. Second, based on estimation of the experimental values of $I_M^{(1)}/I_{0M}$ and $I_M^{(0)}/I_{0M}$, the parameter L for the C set of experiments turns out in accordance with Eqn (2.2.2) to equal $L \approx \pi - 1.2\pi$ that is essentially lower than the cited above magnitude of L. As opposed to Fig. 2, the intensity dips in Figs 8 – 11 were found to be incomplete.

The main reason for the above-mentioned quantitative disparity owes to a departure of the ultrashort pulse shape from a rectangular one along with averaging the power recorded over the time interval of about 0.5 ns with the aid of a measuring apparatus. The matter is that only a portion of ultrashort pulse with a certain intensity $I_{00} \approx I_{0M}^{(0)}$ (or $I_{00} \approx I_M^{(1)}$) is involved in the self-switching act and is transferred to an output of the first (or zeroth) waveguide; the rest of this pulse remains at an output of the first (or zeroth) waveguide. But in recording, the apparatus integrates these fast variations in the ultrashort-pulse power over the time interval $\tau_a \approx 0.5$ ns. And the result is that the envelope dips on an oscillograph screen (Figs 8b, 9b, 10b, 11d) prove to be incomplete (as distinct from Fig. 2), while a magnitude of the gain estimated against an oscillogram (for instance, according to Fig. 10e) appears to be conservative as compared with the theoretical finding due to Eqn (2.2.3)

In the case of D-set oscillograms (Fig. 11d – f), the experimental data points were indicated in Fig. 12 (one's own ultrashort light pulse fits each point in this figure) along with calculated curves [70] (see also Appendix) allowing for integration of the power recorded by an apparatus at hand ($\tau_a \approx 0.5$ ns; furthermore, the pulse 'pedestal' was excluded). Having regard to such integration effect, the theoretical and experimental results correlated not only qualitatively, but quantitatively as well. It stands to reason that the experiment of interest (as also is the previous one) can be used in determining K, Θ, and n_2 (see Appendix).

To verify the absence or presence of a stimulated Raman scattering and to estimate its effect, removable diffraction grating *29* (see Fig. 7) of 300 lines per 1 mm was placed in the path of light beams leaving a waveguide. Correlating pictures on screen *30* and on the oscillograph screen we revealed that the above-mentioned pulse dips and spikes are not accompanied, as a rule, by SRS, i.e. they are brought about at the intensities beyond the threshold value for the Raman effect. In particular, stimulated Raman scattering was not evidenced

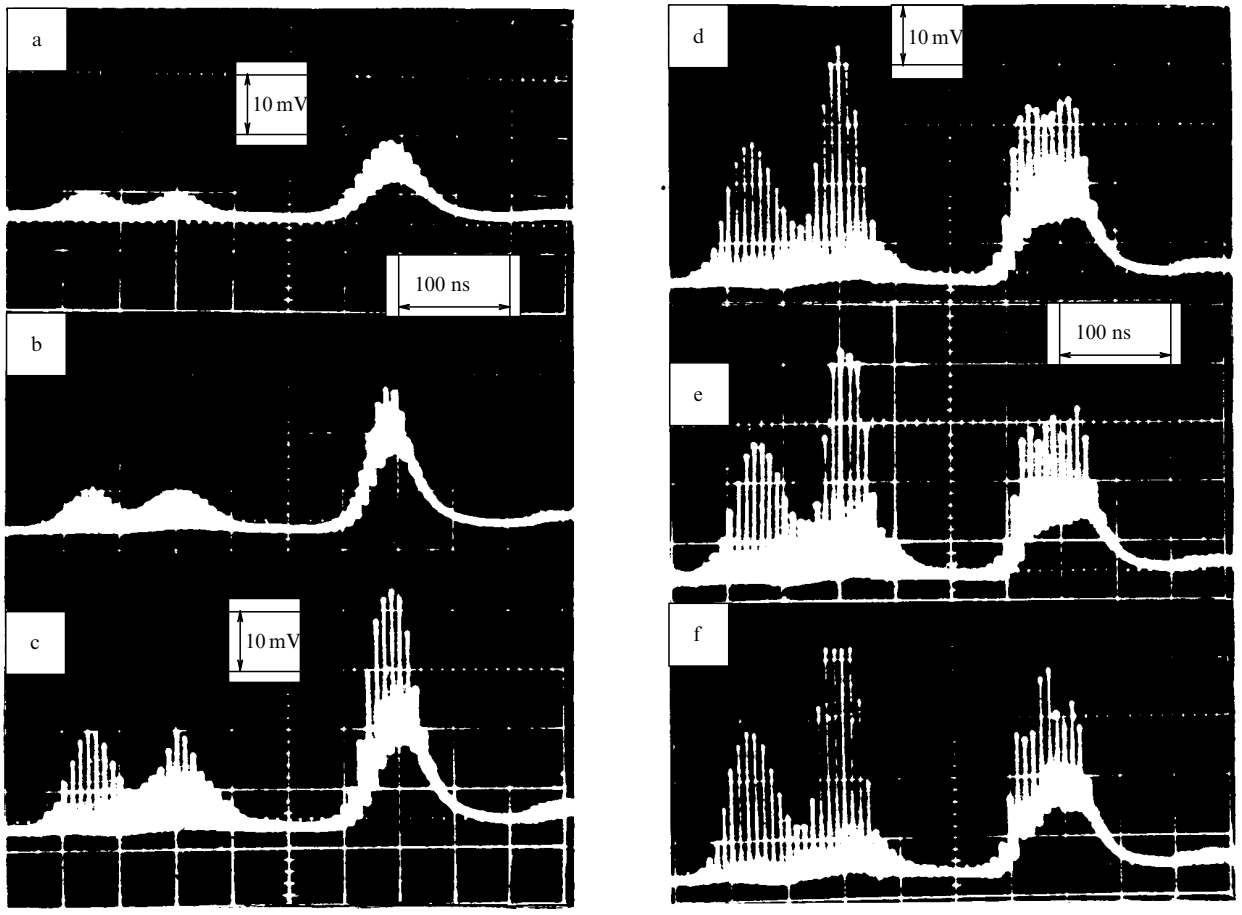

Figure 11. Oscillograms of pulses pertaining to the input signal I_{00} (left pulse train) and output signals I_{1l} (middle train) as well as I_{0l} (right train). Experimental set is labelled as D.

in the sets of experiments involved. Because of this, the pattern mentioned cannot be assigned to the Raman effect. Some other nonlinear phenomena, such as stimulated Brillouin scattering, second harmonic generation, and third harmonic generation were also lacking under conditions of the present experiment.

Relying on the above discussion, we may conclude that the phenomenon of radiation self-switching has been originally observed [45] in the class of UDCW-based systems and the feasibilities of developing the optical transistors on a basis of this phenomenon have been demonstrated as well.

Before long, the analogous experiment was conducted in Ref. [84] and a self-switching phenomenon bracketing UDCWs of different polarizations was also supported. Here, the circularly polarized waves were used. Self-switching of UDCWs possessing orthogonal polarizations has been predicted in Refs [34, 37] and was observed at a later date in Refs [90, 104].

A year odd later, the experiment [45] was repeated in Ref. [92] and the radiation self-switching event in TCOWs was also observed. However, simple interruption of the light-beam portion with the razor blade [92] seems to be less successful solution to the problem of controllable light coupling into one of the waveguide cores as compared to that in Ref. [45]. Prior to development of the light-coupling procedure in Ref. [117], we also have tried to use safety razor for intercepting one of the cores and got the conclusion that this approach does not reliably ensure a controllable radiation injection into one of the optical waveguide cores through light diffraction on the razor's edge.

3.4 Breaking down and shortening of an ultrashort light pulse in its self-switching

The phenomena discussed were first observed in the experiment [46]. The same optic-fibre waveguide and procedure of light coupling into its cores [117] were employed here if compared with Ref. [45]. Two light beams emerged from both the TCOWs were spatially separated (by distance around 5 mm) and directed toward a slit of the high-speed electron-optic (streak) camera. It is clearly seen in the photos (Fig. 13) taken from camera screen and corresponding densitograms (Fig. 14) that at certain intensity ($I_{00} \approx I_{\mathrm{M}}^{(1)}$) of the input pulse there occurs an intensity dip in the central part of one of the output pulses (in Fig. 13 — top) and as if the latter breaks down to two portions. While at the same site of the other output pulse we can view a narrow and an abrupt intensity spike (Fig. 13a, c; Fig. 14a, c). At scarcely larger input intensity ($I_{00} \approx I_{\mathrm{M}}^{(0)}$) the spike discussed above gives way to the dip and the dip — to the spike (Fig. 13b, d; Fig. 14b, d). Durations of the dip and spike comprised less than 6 ps, while the optical waveguide length formed around 1 m, i.e. time of light travel along waveguides came to about 5 ns. By this is meant that the switching time is determined not a time of light travel in TCOW but only a time of optical nonlinearity establishment which in the case of fused quartz comprises a value of order 10^{-14} s.

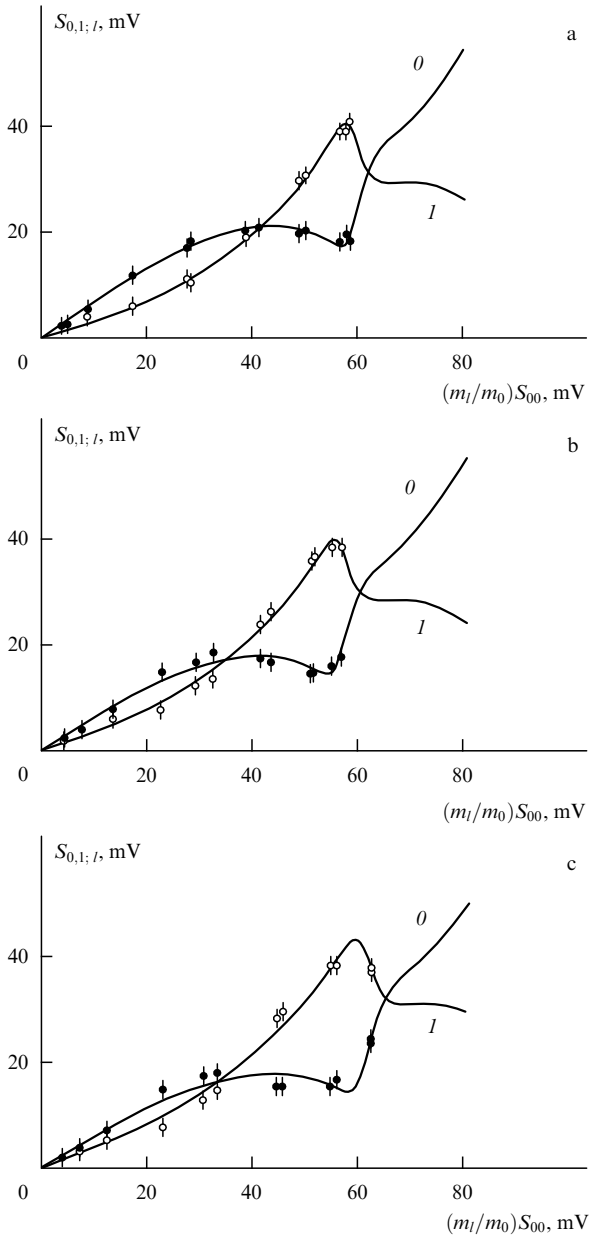

Figure 12. Experimental data points and calculated dependences of output-pulse intensities on input ones with consideration for a pulse integration with respect to time by the apparatus at hand: (a) fits Fig. 11d; (b) fits Fig. 11e; (c) fits Fig. 11f (see Appendix).

Two years later, the experiment analogous to that in Ref. [46] was carried out in Ref. [93]; here, pulses of duration in the 200 fs area were applied to the input and an autocorrelator was employed in recording the output pulses.

3.5 Subsequent experiments

Some attempts at reducing the critical intensity I_{0M} of light self-switching were made in Refs [95, 96] by exploiting exciton resonance in TCOWs fabricated around layered MQW-type structures from A^3B^6 semiconductors possessing pronounced nonlinearity. The severity of the problem lies in the fact that in the vicinity of exciton resonance, where nonlinearity is especially significant, the light absorption becomes excessive. This circumstance compels to reduce the TCOW length l thus depressing the self-switching steepness; by increasing K we can conserve the high steepness of switching but in so doing

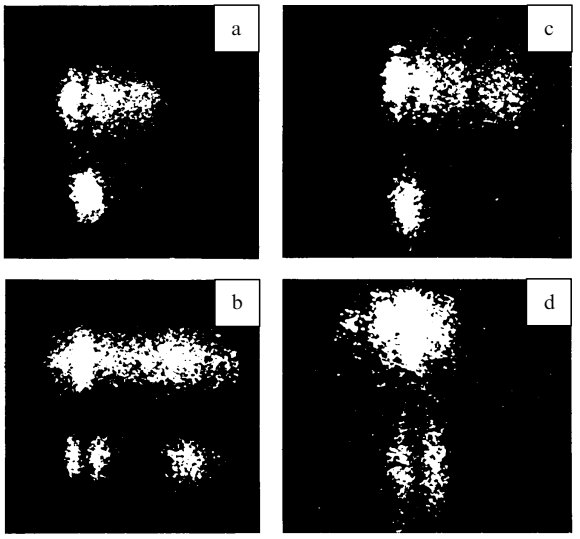

Figure 13. Pulse photographs taken from the camera screen [46]. Two vertically located spots correlate with pulses emerged from two TCOWs.

I_M inevitably rises. Radiation self-switching events have been observed in the strip-type ridge TCOWs (Fig. 15) with light-carrying layer making multiquantum-well structure, which is comprised of the 60-periods GaAs(100 A)/$Al_{0.28}Ga_{0.72}As$(100 A), and with exciton resonance conforming to $\lambda \approx 0.839$ μm [96]. Light coupling into one of the waveguides alone was attained at the expense of employing the zeroth waveguide of length longer by 500 μm than the first waveguide. Two specimens were studied in the experiment [96]. For one of the specimens (ridge height 0.74 μm, interridge gap of about 1 μm) we had $\lambda \approx 0.870$ μm, $\Delta E \approx 53$ meV, $l = 1.2$ mm, $\alpha = 31$ cm^{-1}, transmittance some 1%. For the other one (ridge height 0.74 μm, interridge gap at around 2 μm) the main parameters were as follows: $\lambda \approx 0.878$ μm, $\Delta E \approx 66$ meV, $l = 3.1$ mm, $\alpha = 5$ cm^{-1}. The critical self-switching power $P_M \sim 10$ W was fairly high, in spite of using that structure, while the critical intensity comprised a value of order 10^8 W cm^{-2}, i.e. it was only an order of magnitude lower than in Ref. [45], where a normal optical fibre based on fused quartz was utilized. Since $l \sim 1$ mm in Ref. [96], while $l \sim 1$ m in Ref. [45], then from data presented in Ref. [96] it follows that the MQW nonlinearity was nothing more than four orders of magnitude greater when comparing with optical fibre [45]. On the other hand, from experimental findings of previous work [95], the MQW nonlinearity reached $n_2 = 1.67 \times 10^{-5}$ cm^2 W^{-1}, i.e. it was more than an analogous parameter of fused quartz by seven orders of magnitude. The paradox may be possibly explained by the following reasons. First, continuous radiation was employed in Ref. [95], whereas ultrashort light pulses were under experimentation in Ref. [96]. Because of this, considering 'slowness' of the MQW nonlinearity (without proton bombardment $\tau_{nl} \approx 20$ ns, and with proton bombardment $\tau_{nl} \approx 0.04$ ns [97]) we may assume that nonlinearity in Ref. [96] 'has not managed', and in Ref. [95] 'has managed', to reach its peak (steady) magnitudes, which is why the effective nonlinearity was much pronounced in Ref. [96] as compared to Ref. [95] (even if the tuning out from resonance would be equal in both the works cited [95, 96]). It is conceivable that due to the same reason the effective ratio between MQW

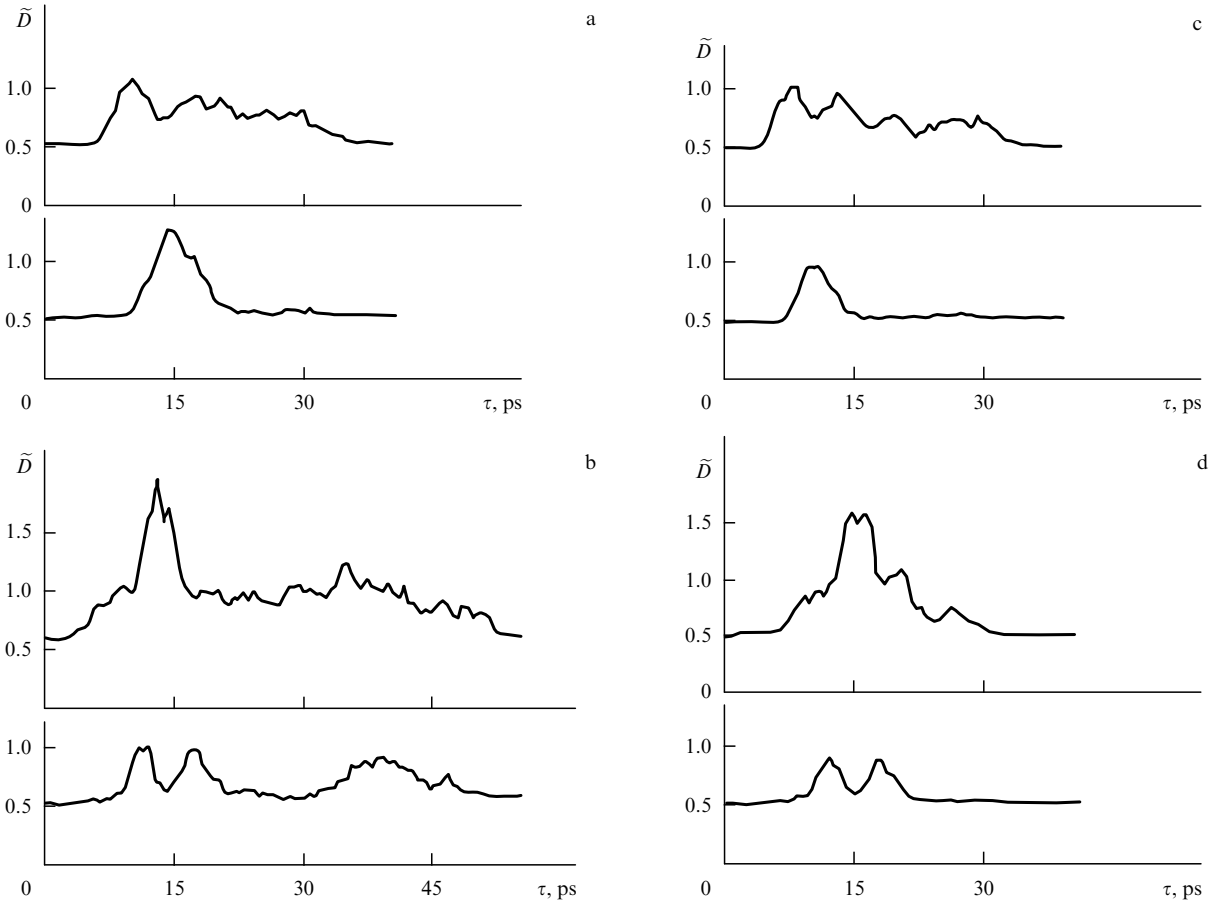

Figure 14. Streak-camera recorded intensity pulse profiles (densitograms) [46] compatible with Fig. 13.

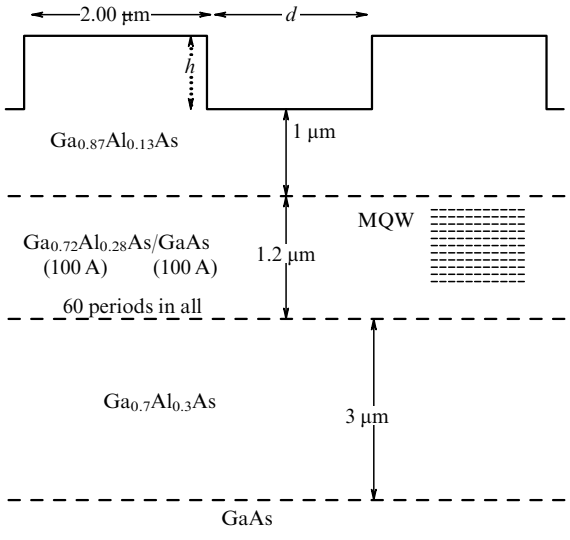

Figure 15. Ridge TCOWs with a light-carrying layer making multiquantum wells from the GaAs(100 A)/$Al_{0.28}Ga_{0.72}As$(100 A) layers [96]. For one of the specimens $d = 1$ μm, $h = 0.74$ μm, whereas for another one — $d = 2$ μm, $h = 0.82$ μm.

nonlinearity [96] and far less inertial optic-fibre nonlinearity [45] under picosecond pulses proved to be not so large as when operating with nanosecond and more lengthy pulses. Second, the authors [95] have come to the exciton resonance: $\Delta E \approx 13$ meV (for $l \approx 2$ mm) much closer and thus have gained much more pronounced nonlinearity and far lower critical intensity (equal to 170 W cm^{-2}) than in Ref. [96]. It has been possible to achieve (in the authors' view [95]) through MQW GaAs/$Al_{0.3}Ga_{0.7}As$ having been resided between optical waveguides and when only weak exponentially falling (in a transverse direction) tail of the field profile has travelled through this medium. In consequence, radiation absorption has decreased in importance and this allowed the exciton resonance to be approximated. Notice that some peculiarities of planar waveguides [95] have been considered earlier in Ref. [94]. However, it is well to bear in mind that the nonlinear waveguide coefficient Θ_j is proportional to the overlap integral taken between the field profile and nonlinearity profile (see Eqn (2.1.8) in [1]), whereas for the scheme of experiment in Ref. [95] this overlapping is smaller if compared with Ref. [96].

Self-switching of radiation with $\lambda = 1.06$ μm was also observed [60, 61] in a dual-core optic-fibre waveguide with end-separated light-carrying cores (Fig. 16). This experiment is analogous to that described in Section 3.3, although the procedure of light coupling into waveguides was to be sure significantly simpler. Employment of TCOWs with end-separated light-carrying cores made just as a controllable injection of radiation into waveguides (or one of them), so the switch association much easier.

Self-switching of one more type of UDCW — unidirectional distributively-coupled waveguide modes — has been experimentally examined, too [98].

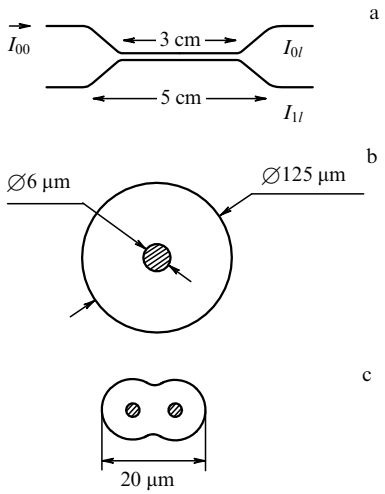

Figure 16. Dual-core optic-fibre waveguide with end-separated cores (a) along with its cross-sectional area at the ends (b) and over the region of tunnel coupling (c) [60, 61].

The experiment on studying the soliton self-switching in TCOWs and other systems involving UDCWs should be forthcoming in the near future. Any research group possessing a solitonic laser could carry out the former. Critical intensity of soliton generation P_s/S has to correlate in this case with the critical intensity of its self-switching. For instance, for optic-fibre waveguide $l \sim 1$ m in length we arrive at $P_{0M} \sim 100$ W [37, 40, 45, 1] and the condition $P_s \approx P_{0M}$ is fulfilled at the pulse length of order 100 fs (see Section 2.3).

3.6 Requirements to the system and pump parameters

To observe the phenomenon of radiation self-switching and to realize devices on its base it is important to think of requirements imposed upon parameters of pumping and UDCW-based system wherein this phenomenon is intended to be detected and used.

3.6.1 Requirements to the system parameters. Scatter in the magnitudes of some parameters (gap between waveguides, width of waveguides, etc.) will show itself in a spread in K values (with relevant dispersion σ_K), which in turn will produce a scatter in I_M values. It is requisite that above scatter fits within the limits of a linear portion of the characteristic. Alternatively, the middle self-switching point M_0 for some parameters coincides with the point M_1 for other parameters [see Eqn (2.2.2)], and radiation self-switching disappears. For this purpose it is essential that, according to estimates, the following inequality is met:

$$\frac{|\sigma_K|}{K} < 8\exp(-L)\,, \tag{3.6.1}$$

so that the relative spread in values of the coupling coefficient ought to be less than inverse gain (k^{-1}). Self-switches with the gain $k \sim 10$ are to be used in optical computers. Such self-switches offer relative scatter in values of gap between waveguides less than 1%. For other parameters of the system (width of waveguides, values of Δn), requirements to a scatter in their values are less strict — no more than a few per cent, because these parameters affect the coupling coefficient to a lesser extent.

3.6.2 On a permissible deviation of TCOWs from perfectness. Constancy of radius a of each of the cores, gap d between the cores, difference between the refractive indices Δn of the core and cladding along the TCOW axis furnishes steadiness of β and K coefficients. In real TCOWs, variations in values of a, d, and Δn cause a spread in values of β and K along the TCOW length which could be characterized by their dispersions σ_β and σ_K. Admissible deviation from the waveguide perfection (i.e. condition of TCOW fitness for an optical transistor) can be formulated in the first approximation in terms of (3.6.1) and

$$\sigma_\beta \ll K\,, \tag{3.6.2}$$

where K is the average coupling coefficient over l. Meaning of inequality (3.6.1) implies that spread in I_{0M} values stemming from scatter in K, may not exceed the size of the linear portion of a self-switching characteristic, so that the relative spread in values of the K coefficient was less than inverse gain (k^{-1}); (3.6.2) follows from the condition of the theory applicability.

In this manner for reducing the effect of TCOW non-ideality (scatter in a, d, Δn parameters) it is more advantageous to operate at small l and large K (matching large I_{0M}), which are rather readily achieved in a discrete optical transistor [43] (see Section 3.2).

3.6.3 Requirements to pumping. Practical realization of the optical transistor in question places heavy demands on the stability of pump intensity I_p. Firstly, the I_p stability is requisite for obviating nonlinear distortion under a signal amplification. Secondly, amplitude of the amplified signal is to be far in excess of that for the amplified 'parasitic' pump variation. In other words, the change-in-signal gain factor ought to be vastly superior to a change-in-pump gain. As a consequence, an optical transistor with coupling of the coherent pump and signal in different waves into a waveguide input (see Refs [55, 56, 62] and Section 4 in Ref. [1]) is obliged to be much more unreceptive to the pump intensity instability than the optical transistor with injection of the incoherent pump and signal in a single wave into a waveguide input (see [34] and Section 3 in Ref. [1]). In the second, most unfavourable, case (see Eqn (2.2.2)) the first condition implies that deviation ΔI_p from a given value $I_p \approx I_{0M}$ meeting a central part of the characteristic-curve linear portion, may not exceed dimensions of the linear portion, i.e.

$$|\Delta I_p| < 32\,\frac{K}{|\Theta|}\exp(-L) \quad \text{or} \quad \left(\frac{\Delta I_p}{I_p}\right)^2 \ll 64\exp(-2L). \tag{3.6.3}$$

In the case of $D = 0$, the pump pulse profile in a discrete optical transistor has to be as close to the rectangular form as possible. Such a profile can be attained in a variety of ways. First, we can do it by using the self-modulation of ultrashort pulses in the nonlinear optical fibre with dispersion through the agency of a delay line with negative dispersion or by employing special transparents [15]. Second, ultrashort pump pulses prior to coupling into the input of a discrete optical transistor may be passed through yet another nonlinear system with UDCWs for purposes of rectangular pulse shaping (and what is more at the expense of the self-switching phenomenon) [43]. The possibility for such a rectangular pulse shaping was demonstrated in Ref. [47] and in Section 2.2 above (see Fig. 2).

3.6.4 On the influence of self-focusing on the UDCW self-switching. Self-focusing event does not wittingly produce any barriers to the light self-switching, if the latter occurs at smaller input power than the self-focusing phenomenon:

$$S\,\frac{4K}{|\Theta|}\,\frac{c\beta}{2\pi}\sim P_{\mathrm{M}}<P_{\mathrm{sf}}\sim\frac{c\beta\lambda^2}{32\pi^2|\Theta|}\,, \tag{3.6.4}$$

where $K=(\lambda\beta/2l)m$, and m is the number of linear light transfers.

Hence it follows that if the waveguide length is not too small:

$$l>\frac{32\pi m\beta S}{\lambda}\sim\frac{32\times\pi\times1.5\times10^{-7}\ \mathrm{cm}^2}{10^{-4}\ \mathrm{cm}}\approx0.15\ \mathrm{cm}, \tag{3.6.5}$$

and specifically $l\geqslant1-2$ mm, then radiation self-switching occurs at smaller power level than the radiation self-focusing. Because the estimate

$$\frac{2\pi a}{\lambda}\sqrt{(\Delta n)2n}\sim2.4$$

holds true, then $\beta S\sim\lambda^2/(\Delta n)$ and (3.6.5) is equivalent to

$$\Delta n>30\,\Theta I_{00}\,. \tag{3.6.6}$$

In this manner condition (3.6.6) implies that the light-induced variation of the refractive index of order ΘI_{00} ought to be considerably less than the difference between the refractive indices of the core and cladding. It was pointed out in Refs [40, 45, 46] that this condition is fulfilled with a major safety margin.

The self-switching phenomenon is able to result in decreasing the waveguide effective cross section and, as a consequence, in increasing the nonlinear coefficient Θ and in reducing $I_{0\mathrm{M}}$.

3.6.5 On the Raman effect. Stimulated Raman scattering in a glass optical waveguide results in a frequency shift of the first Stokes component equal to about 500 cm^{-1}. Once the pump wavelength $\lambda=1.064$ μm, radiation of the wavelength $\lambda=1.12$ μm, 1.18 μm, etc. arise in the optical waveguide. The coupling coefficient K for TCOWs at these wavelengths will have to exceed materially (by 1.5 – 3 times) an appropriate value of K at $\lambda=1.06$ μm, and in consequence it will be significantly higher for Stokes components than K corresponding to the initial pump. Owing to this the Stokes components of propagating light will not be involved in the switching process and they may produce a parasitic background. These components have to be removed from valid signal at the TCOW output by isolating the initial pump radiation with the aid, for instance, of a diffraction grating. Under this spectral selection at the TCOW output, the negative part of SRS will reduce only to a decrease in pump intensity being tantamount (in the first approximation) to the presence of small optical losses in TCOWs. But moderate losses, as shown in Refs [43, 1], would not violate the effect of radiation self-switching.

The part played by SRS is decreased in importance as one passes to short waveguides with UDCWs ($l\leqslant10$ cm) and just these systems are suitable for producing compact devices. At $l\leqslant10$ cm, the portion of pump intensity converted into Stokes components is under 1% and exponentially falls with a decrease in l.

3.6.6 Effect of optical waveguide bends on the light self-switching. Presence of a bend strongly enhances the field 'spreading' out of a waveguide, i.e. it adds to the light field in the mode tail exponentially depending on the curvature radius [4, 6]. Thus, a waveguide bend severely contributes to the field overlapping and then to the waveguide coupling coefficient and consequently the parameter L (and so the self-switching steepness) along with the intensity $I_{0\mathrm{M}}$.

3.6.7 Influence of the waveguide temperature variation and heating on the optical transistor operation. A certain heating of waveguides is unavoidable on passage of radiation through them. It seems likely that such variation of temperature has to affect the operation of a TCOW-based optical transistor to a greater extent than is considered to be the case with other UDCWs as the base, since waves in TCOWs are spatially separated. Let us estimate the degree of this effect.

An optical transistor based on TCOWs operates at the pump intensity close to the critical one: $I_{\mathrm{p}}\approx I_{\mathrm{M}}$; in this case the time-average intensities of waves are equal approximately (see Fig. 1 in Ref. [35] and Ref. [1]) and hence variation of their refraction indices Δn is closely alike, i.e. if TCOWs are identical, then their identicality $(\alpha=\beta_1-\beta_0)$ should be conserved in time. This being so, the displacement of a working point caused by temperature variation may be induced in the main by changing only the coupling coefficient K through the alteration of the waveguide refraction indices or gap d between waveguides. Let us make an estimate of values Δn, Δd for a dual-core optic-fibre waveguide whose losses due to heating-up amount to 1 dB km^{-1}, while these losses are five orders of magnitude lesser for the segment of 1 cm in length, and thus power of the heat released reaches $\Delta Q\sim10^{-4}$ W at the average radiation power 10 W. Heat is gave off for the most part in the waveguide cores of $S\sim10^{-7}$ cm^2 in cross-sectional area, hence at density $\rho\approx2.2$ g cm^{-3}, heat capacity $C\approx0.2$ cal g^{-1} K^{-1}, and thermal conductivity $\tilde{\varkappa}\approx0.003$ cal K^{-1} cm^{-1} s^{-1}, the time of establishment of the thermal equilibrium between a core and cladding $(\tau'\sim\rho CS/\tilde{\varkappa}\sim10^{-5}$ s) is too small. As a consequence, a rise in the core temperature with respect to a cladding is also insignificant and comes to $\Delta T\sim\tau'\Delta Q/Cm\sim10^{-2}$ K. Inasmuch as $\partial n/\partial T\sim10^{-5}$, $\Delta d/d\sim10^{-7}\Delta T$ and the initial (without heating) $\Delta n\approx0.005$, then relative temperature variations of Δn and Δd would run to 2×10^{-5} and 10^{-9}, respectively. Therefore, temperature variations of K and I_{M} over a dual-core optic-fibre waveguide can be neglected [43].

In the case of GaAs-based TCOWs with heat losses of 1 dB cm^{-1}, the temperature variations of K and I_{M} are insignificant as well due to an estimate made in Ref. [43].

4. Optical switching from one frequency to another in a quadratically nonlinear medium

The present section demonstrates the possibility of light switching in the other group of unidirectional distributively coupled waves with an amplitude-dependent coupling coefficient (see Introduction to Ref. [1]). To be specific, the waves with frequencies ω and 2ω propagating through a quadratically nonlinear medium will be analyzed below. These waves were under study over 25 years and it aimed at attaining the maximum value of the radiation power transfer from one wave to another [12 – 14]. The possibility of radiation sudden switching in such systems has been elucidated in Refs [50, 51, 53, 54]. We rendered concrete the

situation when a powerful pump radiation at the frequency ω or 2ω and a weak alternating control signal at the frequency 2ω or ω, respectively, were applied to the input of the quadratically nonlinear medium. It was found that at certain conditions a small change in the signal intensity brings about an abrupt switching of radiation from one frequency to the other at the system output: say, from the frequency 2ω to that of ω, and vice versa. An optical transistor and amplifier can be produced starting from these switchings and corresponding formulae for their gain factors have been derived elsewhere [51, 53, 54].

The switching time is determined by the time of nonlinearity relaxation being of order 10^{-15} s in the case of quadratic nonlinearity. Thus, the speed of response characterizing optical transistors and light switches considered in the present section, is significantly higher (at least by an order of magnitude) than that for analogous devices using the cubical nonlinearity of a medium as the base (see Sections 2 and 3, also Ref. [1]).

It should be emphasized that under conditions accompanying such light switching the complete transformation of optical radiation into the second harmonic is possible already at tuning out of the synchronism [50, 51].

4.1 General formulae

Let us demonstrate the possibility of radiation switching from one frequency (2ω) to the other (ω) (or vice versa) at the output of a medium possessing only quadratic nonlinearity (and when cubic nonlinearity is entirely absent). Light switching is accomplished here by coupling the high-power continuous radiation (pump at the frequency $m\omega$, $m = 1, 2$) and weak controlling signal (at the frequency $\bar{m}\omega$, $\bar{m} = 2/m$) into the entrance of a medium, and by small varying the signal intensity. We shall make it apparent also that small changes of a weak input signal may be transformed into much more pronounced variations of the output intensity with the same frequency, i.e. an optical transistor and amplifier based on this concept might be designed.

Equations for the field amplitudes of the waves propagating at the frequencies ω and 2ω through a quadratically nonlinear medium are well known for a long time [12–14]:

$$\frac{c}{\omega}\beta_1\frac{\mathrm{d}A_1}{\mathrm{d}z} = \mathrm{i}\chi A_2 A_1^* \exp\left(\frac{2\mathrm{i}\Delta z\omega}{c}\right),$$
$$\frac{c}{\omega}\beta_2\frac{\mathrm{d}A_2}{\mathrm{d}z} = \mathrm{i}\chi A_1^2 \exp\left(-\frac{2\mathrm{i}\Delta z\omega}{c}\right), \qquad (4.1.1)$$

where

$$\chi = \mathbf{e}_1\hat{\chi}(\omega = 2\omega - \omega)\mathbf{e}_2\mathbf{e}_1 = \mathbf{e}_2\hat{\chi}(2\omega = \omega + \omega)\mathbf{e}_1\mathbf{e}_1$$

are the convolutions of the quadratic-susceptibility tensor, $\beta_j = n_j\cos^2\sigma_j/4\pi$, σ_j is the angle between a wave vector and the Poynting vector, n_j is the refraction index at the frequency $\omega_j = j\omega$; $\Delta = n_2 - n_1, j = 1, 2$.

Let us introduce real variables $A_j(z) = \rho_j(z)\exp(\mathrm{i}\varphi_j)$, phase difference $\psi(z) = \varphi_2 - 2\varphi_1 + 2\Delta z\omega/c$, and quantities $I_j(z) = |A_j|^2 = \rho_j^2$ proportional to power fluxes $I_j(z) = (c\beta_j/2)I_j(z)$ in the direction of wave vectors (in essence, to the wave intensities). Let two waves be applied to the medium entrance (at $z = 0$): pump wave at the frequency $m\omega$, and the signal with the frequency $\bar{m}\omega$ and with initial parameters:

$$I_m(z = 0) \equiv I_{m0}, \qquad \varphi_j(z = 0) \equiv \varphi_{j0},$$
$$\Psi(z = 0) \equiv \Psi_0 = \varphi_{20} - 2\varphi_{10}. \qquad (4.1.2)$$

We are interested in the magnitudes of wave intensities and phases at the exit of a medium l in length, i.e.

$$I_j(z = l) \equiv I_{jl}, \qquad \varphi_j(z = l) \equiv \varphi_{jl}, \qquad \Psi(z = l) \equiv \Psi_l.$$

With normalized variables in use

$$J_j(z) \equiv \frac{I_j(z)}{I_{m0}}, \qquad J_{j0} \equiv J_j(z = 0), \qquad J_{jl} \equiv J_j(z = l)$$

the solution to a set of equations (4.1.1) and (4.1.2) takes the form [13]:

$$J_{2l} = J_a + (J_b - J_a)\,\mathrm{sn}^2(S, r), \qquad J_{1l} = 1 + J_{\bar{m}0} - J_{2l}, \qquad (4.1.3)$$

where

$$r^2 = \frac{J_b - J_a}{J_c - J_a}, \qquad S = (J_c - J_a)^{1/2}L + F(\mu, r), \qquad L = \frac{\pi l}{l_{nl}}\ ^{\dagger},$$
$$\mu = \arcsin\left(\frac{J_{20} - J_a}{J_b - J_a}\right)^{1/2}, \quad l_{nl} = \frac{\pi c\beta_1\sqrt{c\beta_2}}{\omega\chi\sqrt{2I_{m0}}}, \quad J_a < J_b < J_c$$

are the roots of the equation

$$J(1 + J_{\bar{m}0} - J)^2 - (\Gamma - \tilde{\Delta}J)^2 = 0, \qquad (4.1.4)$$

here

$$\Gamma = J_{10}\sqrt{J_{20}}\cos\Psi_0 + \tilde{\Delta}J_{20}, \qquad \tilde{\Delta} = \frac{\Delta\beta_1\sqrt{c\beta_2}}{\chi\sqrt{2I_{m0}}}.$$

According to findings of Refs [35, 38, 51, 1], the self-switching event happens provided

$$r^2 \approx 1 \quad \text{and} \quad \exp S \gg 1. \qquad (4.1.5)$$

In so doing Eqn (4.1.3) is approximated by the formula (see Ref. [38] and Appendix 2 to Ref. [1]):

$$J_{2l} \simeq \left(\frac{1 - U}{1 + U}\right)^2, \qquad (4.1.6)$$

where $U = r_1^4\exp(2S)/256$.

4.2 Pump wave at the frequency ω, signal wave at the frequency 2ω

In the case of applying the powerful pump wave with the frequency ω ($m = 1$) and a weak controlling signal with the frequency 2ω ($\bar{m} = 2$) to the entrance of a quadratically-nonlinear medium, we have

$$J_{10} = \mathrm{const} = 1, \qquad J_{20} = \frac{I_{20}}{I_{10}} \ll 1,$$
$$J_{jl} = \frac{I_{jl}}{I_{10}}, \qquad \Gamma = \sqrt{J_{20}}\cos\Psi_0 + \tilde{\Delta}J_{20},$$

and Eqn (4.1.4) takes the form

$$J(1 + J_{20} - J)^2 - \left[\sqrt{J_{20}}\cos\Psi_0 + \tilde{\Delta}(J_{20} - J)\right]^2 = 0. \qquad (4.2.1)$$

† Quantity L depends on the pump intensity throughout Section 4.

When $\cos\Psi_0 = \pm 1$, Eqn (4.2.1) possesses an exact solution

$$J_a = J_{20}\,, \qquad J_{b,c} = \left(1 + \frac{J_{20}}{2} + \frac{\widetilde{\Delta}^2}{2}\right) \mp \sqrt{\frac{(J_{20} - \widetilde{\Delta}^2)^2}{4} + \left(\pm\sqrt{J_{20}} - \widetilde{\Delta}\right)^2}\,. \quad (4.2.2)$$

(Notations a, b, c are conventional in this case, because the inequality $J_a < J_b < J_c$ is obeyed only for a part of the values J_{20} and $\widetilde{\Delta}$.)

(1) Let us consider the situation arising under synchronous ($\Delta = 0$, $n_1 = n_2 = n$) interaction of propagating waves. As this takes place, we have

$$J_a \approx J_{20}\cos^2\Psi_0\,; \qquad J_{b,c} \approx 1 \mp \sqrt{J_{20}}\cos\Psi_0\,, \quad (4.2.3)$$

and the parameters entering Eqn (4.1.6) are expressed in the following way:

$$r_1^2 \equiv 1 - r^2 \approx 2\sqrt{J_{20}}\cos\Psi_0 \qquad \left(|r_1^2| \ll 1\right), \qquad S \approx L\,. \quad (4.2.4)$$

It follows from Eqns (4.1.3) and (4.2.4) that at zero signal intensity ($I_{20} = 0$) and $\exp L \gg 1$ we arrive at $J_{2l} = \max \approx 1$ ($I_{2l} = \max \approx I_{10}$), i.e. all the radiation emerges from the system at the frequency 2ω; whereas at very small but nonzero signal intensity [50, 51]:

$$I_{20} \equiv I_{2\mathrm{M}} \approx \frac{64 I_{10}}{\cos^2\Psi_0}\exp(-2L)\,, \quad (4.2.5)$$

inferred from the condition $r_1^4\exp(2S)/256 = 1$, we come up with the relationship $J_{2l} = \min \approx 0$ ($I_{2l} = \min \ll I_{10}$) pointing to the fact that all the radiation leaves the system at the frequency ω (Fig. 17). The situation appears to be paradoxical: in the absence of 2ω-radiation at the system input, almost all the output radiation is found with the frequency 2ω, and if we apply a weak radiation at this frequency to the system input (as though 'wishing the yield of the second harmonic to be enhanced further'), then radiation at this frequency will not be found increased, but suddenly it will disappear on the whole — SHG effect wears off!

By reference to Eqns (4.1.3), (4.2.3), and (4.2.4), let us deduce the gain factor pointing out how many times the change in the output power for each harmonic is larger than variation in the input signal power. Provided $r_1^4\exp(2L)/256 \ll 1$, i.e. at sufficiently low I_{20}, namely, at $I_{20} \ll I_{2\mathrm{M}}$, the gain does not depend on the input intensity of waves with the frequency 2ω and assumes a simple form [50, 51]:

$$k = \frac{\partial I_{2l}}{\partial I_{20}} = 1 - \frac{\partial I_{1l}}{\partial I_{20}} \simeq -\frac{\partial I_{1l}}{\partial I_{20}} \simeq -\frac{\cos^2\Psi_0}{16}\exp 2L\,. \quad (4.2.6)$$

Thus, an optical transistor can be constructed starting from the frequency transformation in a quadratically-nonlinear medium, the gain whereof is defined by formula (4.2.6).

(2) The light switching character is changed drastically on accounting for tuning out of the synchronism ($\Delta \neq 0$) when it is compared with the case of $\Delta = 0$. The gain at the condition $\left|\sqrt{J_{20}} - \widetilde{\Delta}/\cos\Psi_0\right| \ll 8\exp(-L)$ is calculated with the following expression [54]:

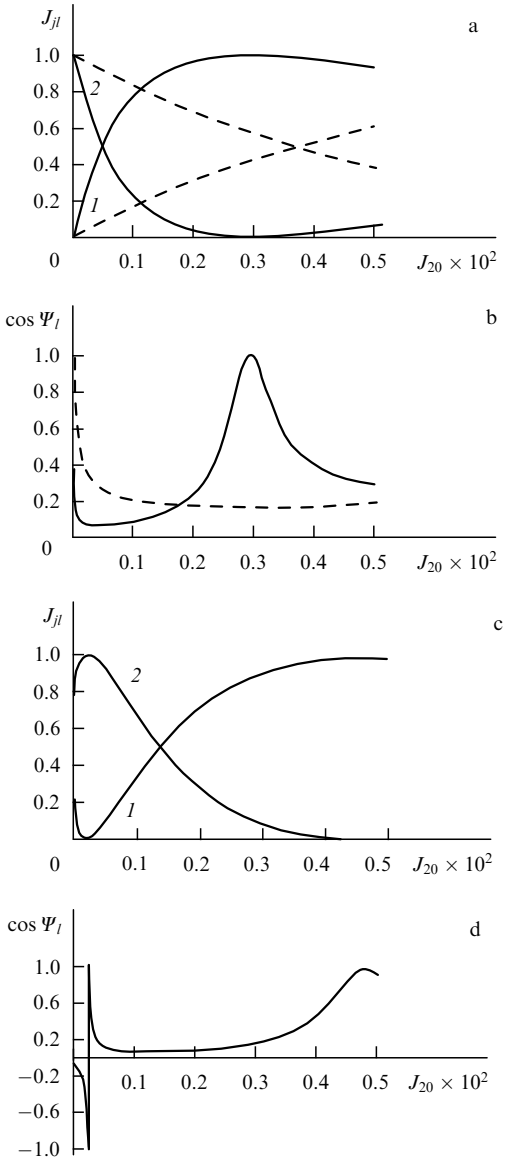

Figure 17. Normalized output intensities $J_{1l} = I_{1l}/I_{10}$ — *1* and $J_{2l} = I_{2l}/I_{10}$ — *2* (a, c), and $\cos\Psi_l$ (b, d) against normalized intensity of the input signal $J_{20} = I_{20}/I_{10}$. Relationship $J_{10} = \mathrm{const} = 1$ holds true. Dashed lines correspond to $L = \pi l/l_{nl} = 4$, whereas solid lines — to $L = 5$. $\Delta = 0$ for (a, b) and $\widetilde{\Delta} = 0.015$ for (c, d) (taken from Ref. [51]).

$$k = \frac{\partial I_{2l}}{\partial I_{20}} \approx -\frac{\partial I_{1l}}{\partial I_{20}} \approx \frac{(\cos^2\Psi_0 + \widetilde{\Delta}^2)\left(\sqrt{1 + \widetilde{\Delta}^2\tan^2\Psi_0} + \widetilde{\Delta}\tan\Psi_0\right)^2}{16(1 + \widetilde{\Delta}^2\tan^2\Psi_0)^3} \times \left(\frac{\widetilde{\Delta}}{\cos\Psi_0}\sqrt{\frac{I_{10}}{I_{20}}} - 1\right)\exp\left(2L\sqrt{1 + \widetilde{\Delta}^2\tan^2\Psi_0}\right). \quad (4.2.7)$$

With the proviso that $|\widetilde{\Delta}| \ll 1$ and $|\cos\Psi_0| \approx 1$, (4.2.7) is somewhat facilitated [51]:

$$k = \frac{\partial I_{2l}}{\partial I_{20}} \approx -\frac{\partial I_{1l}}{\partial I_{20}} \simeq \frac{\cos^2\Psi_0}{16}\left(\frac{\widetilde{\Delta}}{\cos\Psi_0}\sqrt{\frac{I_{10}}{I_{20}}} - 1\right)\exp 2L\,. \quad (4.2.8)$$

If $I_{20} \to 0$, then $|\partial I_{2l}/\partial I_{20}| \to \infty$, i.e. we arrive at the analogue of the 'giant amplification' predicted earlier [37] for the cubically-nonlinear UDCW-based systems with a constant coupling coefficient (see Section 4.4 in Ref. [1]).

The complete transformation of radiation into the second-harmonic wave could be possible during such switching conditions even at the presence of tuning out of the synchronism: when $I_{20} = I_{10}\widetilde{\Delta}^2/\cos^2\Psi_0$, we arrive at $\partial I_{2l}/\partial I_{20} \approx 0$ and $I_{2l} \approx I_{10}$, i.e. a main radiation is virtually transferred to the second-harmonic radiation altogether (even at $\Delta \neq 0$), if, of course, the relationship $\cos\Psi_0 \neq 0$ holds true [50, 51] (see Fig. 14).

The signal intensity $I_{20} \equiv I_{2M}$, at which J_{2l} is minimal, may be deduced from the expression [54]:

$$I_{2M} \approx I_{10}\left[\frac{\widetilde{\Delta}}{\cos\Psi_0} + \frac{8(1+\widetilde{\Delta}^2\tan^2\Psi_0)^2\exp\left(-L\sqrt{1+\widetilde{\Delta}^2\tan^2\Psi_0}\right)}{\sqrt{\cos^2\Psi_0+\widetilde{\Delta}^2}\left(\sqrt{1+\widetilde{\Delta}^2\tan^2\Psi_0}+\widetilde{\Delta}\tan\Psi_0\right)}\right]^2 . \quad (4.2.9)$$

At $|\widetilde{\Delta}| \ll 1$ and $|\cos\Psi_0| \approx 1$ one obtains [54]:

$$I_{2M} \approx I_{10}\left[\frac{\widetilde{\Delta}}{\cos\Psi_0} + \frac{8\exp(-L)}{|\cos\Psi_0|}\right]^2 . \quad (4.2.10)$$

The operational regime of an optical transistor (i.e. linear amplification) under the conditions $\Delta \neq 0$ and $\Delta > 0$ is accomplished only within the range $I_{10}\widetilde{\Delta}/\cos^2\Psi_0 < I_{20} < I_{2M}$.

Results of the analysis of Eqns (4.2.5)–(4.2.10) are confirmed by the findings (see Fig. 17) evident from the numerical solution to the set of equations (4.1.1) with initial conditions (4.1.2).

Let us make an estimate. Assume that the main radiation with the frequency ω and intensity $I_{10} \approx 2 \times 10^7$ W cm^{-2} is coupled into the KTP crystal of length $l = 1$ cm, nonlinearity $\chi \approx 3 \times 10^{-8}$ esu and $n = 1.78$ coincidentally with a weak control signal at the frequency 2ω with $\Delta = 0$, $\Psi_0 = 0$, and $\beta_1 = \beta_2 = n/4\pi$. In this case

$$\widetilde{I}_{10} = \frac{8\pi I_{10}}{cn} \approx 9 \times 10^4 \text{ erg cm}^{-3},$$

$$l_{nl} = \frac{\lambda n}{8\pi\chi\sqrt{\widetilde{I}_{10}}} \approx 0.8 \text{ cm}, \qquad L \approx 1.25\pi .$$

In compliance with (4.2.6) $dI_{1l}/dI_{20} \approx 160$. The signal gain in the 'giant amplification' regime ($\Delta \neq 0$) is still more by a factor of $\widetilde{\Delta}\sqrt{I_{10}/I_{20}}$.

4.3 Pump wave at the frequency 2ω, signal wave at the frequency ω

In the event of applying the high-power pump wave at the frequency 2ω ($m = 2$) and a control signal at the frequency ω ($\bar{m} = 1$) to the input of a quadratically-nonlinear medium, namely,

$$J_{20} = \text{const} = 1, \qquad J_{10} = \frac{I_{10}}{I_{20}} \ll 1, \qquad J_{jl} = \frac{I_{jl}}{I_{20}},$$

$$\Gamma = J_{10}\cos\Psi_0 + \widetilde{\Delta},$$

($J_{10} \ll 1$), Eqn (4.1.4) takes the form

$$J(1+J_{10}-J)^2 - \left[J_{10}\cos\Psi_0 + \widetilde{\Delta}(1-J)\right]^2 = 0 . \quad (4.3.1)$$

Notice that with the proviso $\cos\Psi_0 = \pm 1$, the exact solution to Eqn (4.3.1) could be gained as in the previous case (see Section 3.2):

$$J_b = 1, \qquad J_{a,c} = \frac{1+\widetilde{\Delta}^2+2J_{10}}{2} \mp \sqrt{\frac{(1-\widetilde{\Delta}^2)^2}{4} + J_{10}(\pm 1-\widetilde{\Delta})^2} . \quad (4.3.2)$$

(As before, the root notations are conventional.)

(1) Let us consider firstly synchronous interaction of propagating waves ($\Delta = 0$, $n_1 = n_2 = n$) when the roots of Eqn (4.3.1) are calculated approximately by the following formulae:

$$J_a \approx J_{10}^2\cos^2\Psi_0, \qquad J_{b,c} \approx 1 + (1 \mp \cos\Psi_0)J_{10}, \quad (4.3.3)$$

and the parameters r_1^2, S entering (4.1.3) equal [53, 54]:

$$r_1^2 \approx 2J_{10}\cos\Psi_0, \qquad S \approx L + \ln\frac{4}{\sqrt{2J_{10}(1+\sin\Psi_0)}} . \quad (4.3.4)$$

If expressions (4.3.3) and (4.3.4) are substituted into Eqn (4.1.3), then we arrive at the conclusion that J_{2l} is maximal and $I_{2l} = I_{20}$ with the zero signal ($I_{10} = 0$) and the inequality $\exp L \gg 1$ held true, i.e. almost all the output radiation is concentrated in the second-harmonic wave. The input intensity $I_{10} = I_{1M}$ at which J_{2l} comes to nought and nearly all output radiation possesses the frequency ω, is determined by the relationship $r_1^4\exp(2S)/256 = 1$ from which one readily obtains [53, 54]:

$$I_{1M} \approx \frac{8I_{20}}{1-\sin\Psi_0}\exp(-2L) . \quad (4.3.5)$$

The gain factor at $I_{10} \ll I_{1M}$ does not depend on the input intensity of the wave with the frequency ω and simply appears as [53, 54]:

$$\frac{\partial I_{2l}}{\partial I_{10}} = 1 - \frac{\partial I_{1l}}{\partial I_{10}} \approx -\frac{\partial I_{1l}}{\partial I_{10}} \approx -\frac{1-\sin\Psi_0}{2}\exp 2L . \quad (4.3.6)$$

Provided $\sin\Psi_0 = 1$, the radiation switching effect wears out: $\partial I_{2l}/\partial I_{10} = 0$.

Consequently, it is possible to devise an optical transistor on the base of the parametric double-frequency interaction in a quadratically-nonlinear medium. The gain factor of this transistor is deduced from Eqn (4.3.6) and proves to be sixteen-fold higher (at $\sin\Psi_0 = -1$) than that in the event of coupling into the system input the pump wave at the frequency ω and the signal at the frequency 2ω [see Eqn (4.2.6)].

(2) Tuning out of the synchronism ($\Delta \neq 0$) does not tangibly alters the switching behaviour (at least for $\widetilde{\Delta} \ll 1$). Parameters entering Eqn (4.1.4) can be expressed at $J_{10} \ll 1$ in the following way [54]:

$$J_a \approx \widetilde{\Delta}^2 + 2\widetilde{\Delta}(\cos\Psi_0 - \widetilde{\Delta})(1-\widetilde{\Delta}^2)^{-1}J_{10},$$

$$J_{b,c} \approx 1 + (1 \mp \cos\Psi_0)(1 \mp \widetilde{\Delta})^{-1}J_{10},$$

$$r_1^2 \approx \frac{2(\cos\Psi_0 - \widetilde{\Delta})J_{10}}{(1-\widetilde{\Delta}^2)^2}\,,$$

$$S \approx L\sqrt{1-\widetilde{\Delta}^2} + \ln\frac{4(1-\widetilde{\Delta}^2)}{\left\{2J_{10}\left[1+(1-\widetilde{\Delta}^2)^{1/2}\sin\Psi_0 - \widetilde{\Delta}\cos\Psi_0\right]\right\}^{1/2}}\,. \tag{4.3.7}$$

By application of just written relationships (4.3.7) we can derive from Eqn (4.1.3) that the middle switching point M_1 is somewhat shifted (as compared to the case of $\Delta = 0$) and the signal intensity corresponding to that point is calculated by the formula [54]:

$$I_{1M} \approx \frac{8I_{20}(1-\widetilde{\Delta}^2)^2\left[1+(1-\widetilde{\Delta}^2)^{1/2}\sin\Psi_0 - \widetilde{\Delta}\cos\Psi_0\right]}{(\cos\Psi_0 - \widetilde{\Delta})^2} \times \exp\left(-2L\sqrt{1-\widetilde{\Delta}^2}\right), \tag{4.3.8}$$

and the gain at $I_{10} \ll I_{1M}$ takes the form [54]:

$$\frac{\partial I_{2l}}{\partial I_{10}} \approx -\frac{(\cos\Psi_0 - \widetilde{\Delta})^2\exp\left(2L\sqrt{1-\widetilde{\Delta}^2}\right)}{2(1-\widetilde{\Delta}^2)^2\left[1+(1-\widetilde{\Delta}^2)^{1/2}\sin\Psi_0 - \widetilde{\Delta}\cos\Psi_0\right]}\,. \tag{4.3.9}$$

When $\Psi_0 = 0, \pi$, one arrives at [53]

$$\frac{\partial I_{2l}}{\partial I_{10}} \approx -\frac{(1-\widetilde{\Delta})\exp\left[2L(1-\widetilde{\Delta}^2/2)\right]}{2}\,.$$

Thus, tuning out of the synchronism somewhat decreases the gain factor without disturbing the characteristic linearity [53]. Therein lies a notably essential dissimilarity from the case of $I_{20} \ll I_{10}$ discussed above in Section 4.2 and Ref. [51].

Since tuning out of the synchronism does not disturb a linear character of the amplification curve and affects the gain factor with relative weakness, and in addition to that the gain at $\Delta = 0$ proves to be much higher than in the case of $I_{20} \ll I_{10}$ (8 times more at $\sin\Psi_0 = 0$, and 16 times more at $\sin\Psi_0 = -1$), then from the standpoint of an optical transistor construction the limiting case $I_{20} \gg I_{10}$ offers far more promise [53] when compared to the reverse case of $I_{20} \ll I_{10}$.

Figure 18 displays the results of the analysis applied to Eqns (4.3.5) – (4.3.9).

Let us consider below the numerical example [53]. Assume that pump radiation with the wavelength $\lambda = 0.53$ μm and intensity 8×10^7 W cm^{-2} is coupled into the KTP crystal of length $l = 1$ cm (and with $\chi \approx 3 \times 10^{-8}$ esu, $n = 1.78$) at an angle of synchronism (phase-matching). The above intensity is attained at a relatively minor average power ($\simeq 10$ W) through radiation focusing into the crystal centre and using the continuous sequence of ultrashort ($\simeq 100$ ps) light pulses with repetition interval around 10 ns and peak power close to 100 W; the temporal profile of pulses has got to be near-rectangular in shape. Under these conditions $l_{nl} \approx 0.8$ cm, $L \approx 1.25\pi$. Synchronous with the pump wave, a weak alternating control signal (coherent with a pump) with the wavelength $\lambda = 1.06$ μm is injected into the crystal. The thin (≈ 200 μm) glass plate is interposed in the path of signal and pump waves in front of a crystal input and the Ψ_0 value close to $\pi/2$ is matched by making a turn of this plate. In compliance with (4.3.6), the signal modulation would be enhanced by the factor 2600.

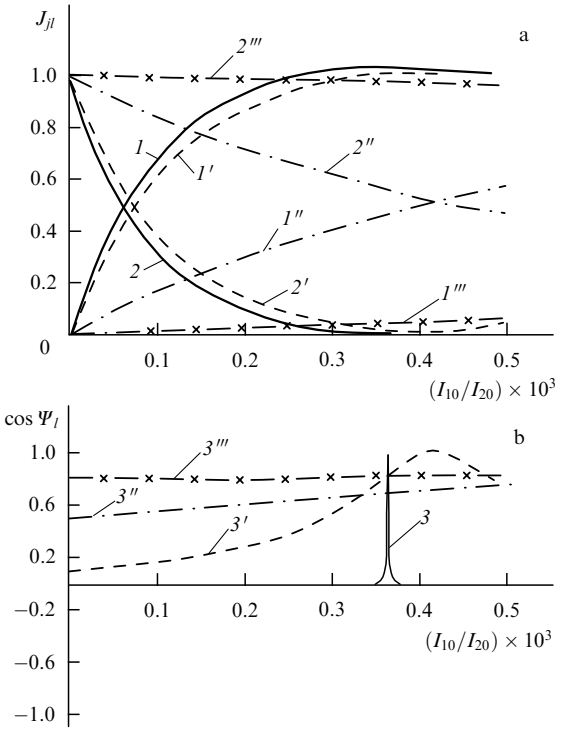

Figure 18. Normalized output intensities $J_{1l} = I_{1l}/I_{20}$ — $1-1'''$ and $J_{2l} = I_{2l}/I_{20}$ — $2-2'''$ (a), and $\cos\Psi_l$ (b) against normalized intensity of the input signal $J_{10} = I_{10}/I_{20}$. Relationship $J_{20} = \text{const} = 1$ holds, $L = \pi l/l_{nl} = 4\pi(\omega/c)l\chi\widetilde{I}_{20}^{1/2} = 5$: $\Delta = 0$ ($1-3$); $\widetilde{\Delta} = \Delta n/4\pi\chi\widetilde{I}_{20}^{1/2} = 0.1$ ($1'-3'$), 0.5 ($1''-3''$), 0.8 ($1'''-3'''$) (taken from [53]).

4.4 On the wave autosynchronization

The switching of waves is accompanied by their autosynchronization and abrupt change of the wave phase difference (Fig. 17b, d and Fig. 18b) on small signal variation [51, 53, 54]. This phenomenon attendant to radiation self-switching is organically connected with the latter, just as the autosynchronization and abrupt change of the phase difference accompanies self-switching of UDCWs with a linear coupling coefficient [38, 37, 1]. In essence, the abrupt change of the wave phases (sharp phase shift) does produce radiation switching. Two years after the papers [51, 53] issued, just mentioned conclusion concerning the sharp phase shift [51, 53, 54] was experimentally supported in Ref. [118], and six years later — in Refs [119, 120].

Seven years after the publications [50, 51, 53], the idea of radiation self-switching was confirmed in Ref. [121].

4.5 Light switching by phase variation

One may switch the radiation at the system output by varying the input phase of a signal (or a pump). Dependences of J_{jl} and $\cos\Psi_l$ on the initial phase difference Ψ_0 for some magnitudes of the pump intensity can be found in Refs [50, 52, 53] and are given in Fig. 19. The dependence of J_{jl} on Ψ_0 is analogous to that displayed in Fig. 14 [1] and pertaining to UDCW-based optical waveguide with a linear coupling coefficient.

Strong dependence of the output phase difference on the input one may be used also for steep amplification of the phase shift (it is small at the input and high at the output), i.e.

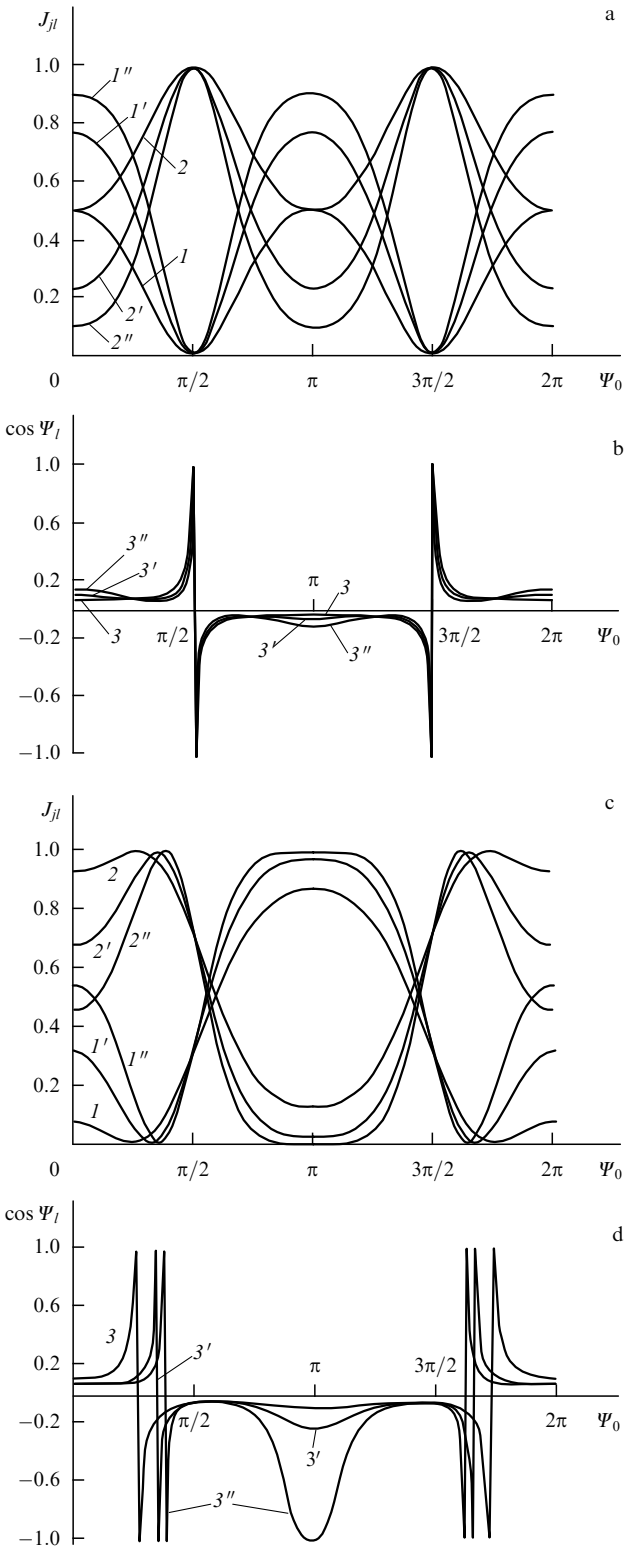

Figure 19. Normalized output intensities J_{1l} ($1-1''$) and J_{2l} ($2-2''$) (a, c), and $\cos\Psi_l$ (b, d) against initial phase difference Ψ_0 at $L = 5$ for the cases of synchronous $\Delta = 0$ (a, b) and asynchronous $\tilde{\Delta} = 0.015$ (c, d) wave interactions at $J_{20} = 0.5 \times 10^{-3}$ ($1-3$), 10^{-3} ($1'-3'$), 1.5×10^{-3} ($1''-3''$); $J_{10} = \text{const} = 1$ (taken from [51, 54]).

for abrupt enhancement of phase modulation. This phenomenon may in turn find application to broadening of the frequency spectrum (chirp) and, as a consequence, to a pulse shortening.

4.6 On the self-switching of other UDCWs with nonlinear coupling coefficients

We have detailed in the foregoing the problem of light self-switching for UDCWs with nonlinear coupling coefficient by treating as an example the system with UDCWs at the frequencies ω and 2ω, which were propagating through a quadratically-nonlinear medium.

Analogous switching effect may occur under conditions of accompanying four-wave interaction in a medium with cubic nonlinearity Θ, when two high-power plane reference waves with A_1 and A_2 amplitudes interact with a couple of relatively weak signal waves of amplitudes A_3 and A_4; $A_j(z = 0) \equiv A_{j0}$, $A_j(z = l) \equiv A_{jl}$ [52]. Here, wave frequencies may differ, i.e. the A_j-amplitude wave possesses the frequency ω_j. To estimate the switching steepness, one can rely on the results obtained in Ref. [122], whilst the switching phenomenon itself has not been discussed in the work cited. If one of the signal waves is generated as a result of such interaction ($A_{40} = 0$), then for optimal tuning out of synchronism the variation of the output signal intensity would be

$$k = \frac{\partial|A_{4l}|^2}{\partial|A_{30}|^2} \simeq \exp\left(\frac{\Theta|A_{10}A_{20}|2\pi l}{\lambda}\right)$$

times as large as the signal intensity change at the system input [52]. In consequence, an optical transistor can be constructed on the basis of this interaction. The interaction behaviour reminds one of that of waves with orthogonal polarizations and the coefficient of linear coupling equal to zero (see [1]). This can be traced to a similarity of equations governing these processes. As pointed out in Section 4.11 [1] and Ref. [72], self-switching of UDCWs of orthogonal polarizations with equal-to-zero linear coupling coefficient constitutes essentially a particular case of the degenerate four-wave interaction when all the waves possess a single frequency and their polarizations coincide in pairs (two waves are polarized along the x axis, while two others — along the y axis). This self-switching phenomenon can also form the basis of a logic element development.

Analogous logic elements are constructible starting from accompanying stimulated Raman scattering effect as well [123].

It seems likely that the phenomenon of light self-switching involving UDCWs with a nonlinear coupling coefficient and the possibility of developing an optical transistor on its base have been first predicted in Ref. [34], where UDCWs were considered in a medium with quadratic and cubic nonlinearities (see also [48]).

4.7 On the synchronism of coupled waves

Interaction of unidirectional distributively-coupled waves (with the constant coupling coefficient K) between themselves opens up new fields of use not only in optical transistor constructing but also in a synchronous conversion of frequency. It was demonstrated in Refs [124–126] that some previously unknown types of phase synchronism referred to as 'coupled-wave synchronisms' (CWS) [126] appear to be possible under frequency conversion and, in particular, under second-harmonic generation in the conditions of UDCW interaction (with the coupling coefficient K). While the present review article deals with the problems of UDCW self-switching, it is not out of place to discuss the CWS peculiarities as well. Firstly, because the latter are connected with a nonlinear UDCW interaction and, secondly, for CWS

enable, in my opinion, the frequency conversion efficiency to be enhanced and, consequently (in accordance with findings presented in Sections 4.2 and 4.3), good opportunities for UDCW self-switching to be provided. The basic possibility of exhibiting such synchronisms is seen by referring to the following reasons. Linear interaction of UDCWs produces splitting of each wave into the fast and slow components, i.e. the refraction index of each wave is split into two effective quantities [3–8]:

$$\beta_{jk}^{(+)} = \beta_{jk} \pm \gamma_j$$

(where $\gamma_j = (\alpha_j^2/4 + K_j^2)^{1/2}$, $j = 1, 2$ is an ordinal number of the frequency $\omega_j = j\omega$, k is an ordinal number of the wave), each being consistent with the field type of its own. Thus, if waves of different types (slow and fast components) are involved in the nonlinear interaction at various frequencies (say, ω and 2ω), then the splitting discussed permits, in certain situations, the medium frequency dispersion to be compensated and the synchronism condition to be fulfilled.

When generating the second harmonic under conditions of 'coupled-wave synchronism'

$$p\gamma_1 - q\gamma_2 = \Delta \tag{4.7.1}$$

(where $p = 0, \pm 1$, $q = \pm 1$, and $\Delta = (\beta_{21} - \beta_{11} + \beta_{20} - \beta_{10})/2$ is the dispersion), amplitudes of the harmonics rise proportional to the distance z passed by the waves [124–126]: $|A_{20}| \propto zC_{p,q}^{(0)}$, $|A_{21}| \propto zC_{p,q}^{(1)}$.

Effective nonlinear susceptibilities (ENS) $C_{p,q}^{(0,1)}$ depend now on the coefficients K_j of a wave linear coupling and the parameters α_j of tuning out. These ENS have been analyzed in detail elsewhere [125–129] under a variety of relationships between α_j and K_j. They are dependent on the overlap integrals of modes pertaining to different frequencies.

There appear six variants of a synchronism in accordance with possible combinations of p and q indices in Eqn (4.7.1).

Under the synchronism 1 ($p = 1$, $q = -1$: $\gamma_1 + \gamma_2 = \Delta$, $\beta_{1k}^{(+)} = \beta_{2k}^{(-)}$), the type '+'-field of the frequency ω, i.e. slow component of the basic wave, synchronizes with the type '−'-field of the frequency 2ω, i.e. fast component of the second harmonic. Under the synchronism 2 ($p = 0$, $q = -1$: $\gamma_2 = \Delta$, $\beta_{1k}^{(+)} + \beta_{1k}^{(-)} = \beta_{2k}^{(-)}$), slow and fast components of the basic wave generate the fast field component at the doubled frequency. Interpretation of the rest four CWSs is analogous to that given above.

The original character of CWS at hand [126] was intimated in Ref. [130], but as the trouble with this idea the authors of [130] pointed to a lesser overlap integral taken over profiles of the basic wave and a wave harmonic (and, in consequence, to a lesser effectiveness of SHG) as compared to the event with a single optical waveguide. However, that is not entirely the case. The matter is that due to perturbation theory the influence of the adjacent waveguide makes itself evident (in the first approximation) only in the change of the propagation constant, whereas the field profile remains unvaried in this approximation. On the contrary, appearance of CWS is liable to permit (at sufficiently large coupling coefficients) a synchronization of the zero-order wave-mode interaction at different frequencies (as verified by numerical results [126, 128, 129]), while in solitary waveguides synchronism is attained between wave modes of various orders possessing substantially lesser overlap integrals. One such advantage of CWS, where frequency conversion in optical waveguides is involved, over known synchronisms implies that we can tune smoothly in synchronism [126, 127] either mechanically [126] (by varying distance between waveguides) or electrooptically [127]. Another advantages of CWS for light beams propagating through TCOWs have been demonstrated in Refs [126, 128].

Notice that CWS were examined experimentally and used successfully in measuring the TCOW coupling coefficient [131].

It would be interesting to know that results in Ref. [126] were patented in the Netherlands [132] ten (!) years later (among other things the possibility of smooth mechanical tuning in synchronism predicted in Ref. [126]).

Some other questions of repeating the results found in Refs [37, 41, 43] within a few years of their publications and without any citation have been broached in Ref. [133].

4.8 Radiation self-switching in quadratically nonlinear TCOWs

Switching of radiation from one frequency to the other is also possible in quadratically nonlinear TCOWs, where light switching from one waveguide to another can occur as well.

Reduced equations governing amplitudes of two UDCWs in a quadratically nonlinear medium with the coupling coefficients dependent on and independent of the wave amplitudes have been derived and analyzed in Ref. [128]:

$$\begin{aligned}
&\mathrm{i}\beta_{10}\frac{\mathrm{d}A_{10}}{\mathrm{d}z_n} + K_1 A_{11}\exp(\mathrm{i}\alpha_1 z_n) = -P_{10}\,,\\
&\mathrm{i}\beta_{11}\frac{\mathrm{d}A_{11}}{\mathrm{d}z_n} + K_1 A_{10}\exp(-\mathrm{i}\alpha_1 z_n) = -P_{11}\,,\\
&\mathrm{i}\beta_{20}\frac{\mathrm{d}A_{20}}{\mathrm{d}z_n} + 2K_2 A_{21}\exp(2\mathrm{i}\alpha_2 z_n) = -P_{20}\,,\\
&\mathrm{i}\beta_{21}\frac{\mathrm{d}A_{21}}{\mathrm{d}z_n} + 2K_2 A_{20}\exp(-2\mathrm{i}\alpha_2 z_n) = -P_{21}\,,
\end{aligned} \tag{4.8.1}$$

where

$$P_{1k} = \sum_{m,l} \chi_{kml}^{(1)} A_{2m} A_{1l}^{*} \exp(\mathrm{i}\delta_{mlk} z_n)\,,$$

$$P_{2m} = \sum_{k,l} \chi_{mkl}^{(2)} A_{1k} A_{1l} \exp(-\mathrm{i}\delta_{mlk} z_n)\,;$$

$$\delta_{mkl} = 2\beta_{2m} - \beta_{1k} - \beta_{1l}\,; \qquad z_n = \frac{z\omega}{c}\,;$$

$k, l, m = 0, 1$ are the wave numbers; K_j is the coefficient of coupling between '0' and '1' waves at the frequency $j\omega$, which depends on the type of UDCW. The terms entering P_{1k} and P_{2m} conform to six channels of nonlinear wave interaction, each being characterized by its own nonlinear coefficient $\chi_{kml}^{(1)}$ or $\chi_{mkl}^{(2)}$.

In the case of TCOWs, only zeroth coefficients may be taken into account due to exponentially dropping field profile:

$$\chi_{000}^{(1)} = \chi_0\,, \qquad \chi_{111}^{(1)} = \chi_1\,, \qquad \chi_{000}^{(2)} = \chi_0\,, \qquad \chi_{111}^{(2)} = \chi_1\,,$$

while the remaining ones may be put equal to zero: $\chi_{kml}^{(1)} = \chi_{mkl}^{(2)} = 0$, unless all the indices are equal between themselves. In this event, Eqn (4.8.1) integrates to the

following expressions [54]:

$$E = \beta_{10}I_{10} + \beta_{11}I_{11} + \beta_{20}I_{20} + \beta_{21}I_{21}\,,$$
$$G = 2K_1\sqrt{I_{10}I_{11}}\,\cos\psi_1 + 2K_2\sqrt{I_{20}I_{21}}\,\cos\psi_2 + \chi_0 I_{10}\sqrt{I_{20}}\,\cos\psi_{20} + \chi_1 I_{11}\sqrt{I_{21}}\,\cos\psi_{21} + \beta_{10}^2 I_{10} + \beta_{11}^2 I_{11} + \beta_{20}^2 I_{20} + \beta_{21}^2 I_{21}\,, \qquad (4.8.2)$$

where

$$\psi_1 = \varphi_{11} - \varphi_{10} + \alpha_1 z_n\,, \quad \psi_2 = \varphi_{21} - \varphi_{20} + 2\alpha_2 z_n\,,$$
$$\psi_{2k} = \varphi_{2k} - 2\varphi_{1k} + 2\Delta_k z_n\,, \quad \Delta_1 = \beta_{21} - \beta_{11}\,,$$
$$\Delta_0 = \beta_{20} - \beta_{10}\,, \quad \alpha_1 = \beta_{11} - \beta_{10}\,, \quad \alpha_2 = \beta_{21} - \beta_{20}$$

and real amplitudes and phases of the waves have been introduced: $A_{jk} = \rho_{jk}\exp\mathrm{i}\varphi_{jk}$; $I_{jk} = \rho_{jk}^2$, $I_{jk}(z=0) \equiv I_{jk;0}$.

Moreover, when considered only synchronously interacting field types at the frequencies ω and 2ω (for CWS), analysis of radiation self-switching from one frequency to the other by using Eqn (4.8.1) manages to perform [73] and it is analogous to that made in Sections 4.1–4.3.

Under the synchronism 2, the complete self-switching is possible, since both the field types at the frequency ω experience interaction and, when merging with each other, they might be fully converted to the second harmonic (Fig. 20).

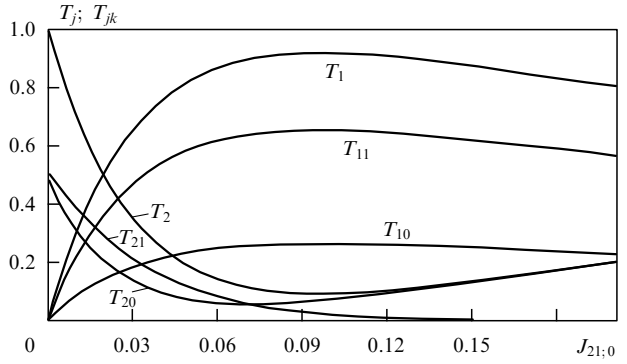

Figure 20. Plots of coefficients of the power transfer at the frequencies $j\omega$ ($j = 1, 2$) by the solitary k-th waveguide ($k = 0, 1$): $T_{jk} = I_{jk}/(I_{10;0} + I_{21;0})$ and both the TCOWs: $T_j = T_{j0} + T_{j1}$ versus functions of normalized intensity of the input signal with the frequency 2ω: $J_{21;0} \equiv I_{21;0}/I_{10;0}$ under synchronism condition (4.7.1) at $p = 0$, $q = -1$ and the following parameters: $K_2 = \Delta = \Delta_0 = \Delta_1$, $\alpha_j = 0$, $K_1 = 4K_2$, $\chi = \chi_0 = \chi_1$, $\chi\sqrt{I_{10;0}}\,l\omega/c = \widetilde{L}\sqrt{2} = 5$.

Let us assume that the synchronism-2 condition is met, 2ω-frequency signal is coupled into the first waveguide, and ω-frequency pump wave is injected into the zeroth waveguide. Besides, if nonidenticality of TCOWs is small: $(\alpha_1/K_1)^2 \ll 1$, and their length appears to be reasonably large: $\exp\widetilde{L} \gg 1$, then the intensity of the second harmonic at the system output may be estimated as follows [73]:

$$I_{2;l} \equiv I_2(z=l) \approx I_{10;0}\,J_{2;l}^{(q)} \approx I_{10;0}\left(\frac{1-U}{1+U}\right)^2, \qquad (4.8.3)$$

where expressions for $\widetilde{L}$, $J_{2;l}^{(q)}$, $J_{2;0}^{(q)}$, $\psi_0^{(q)}$ can be found in Ref. [73], $I_j = I_{j0} + I_{j1}$, and

$$U = u + \frac{J_{2;0}^{(q)}\cos^2\psi_0^{(q)}\exp(2\widetilde{L})}{64}\,, \qquad u \equiv \left(\frac{\alpha_1}{16\gamma_1}\right)^2\exp 2\widetilde{L}\,.$$

Formula (4.8.3) is of a radically different kind from analogous formulae (4.1.6), (4.2.4) in that the additional term u enters the numerator and denominator of the former. This suggests that (as opposed to [51]) $I_{1;l}$ is allowed to be commensurable with $I_{2;l}$ or else considerably in excess of it even at zero input signal, if TCOWs are nonidentical ($\alpha_1 \neq 0$). In the absence of tunnel coupling ($K_j = 0$), namely, in the conditions taken up in Sections 4.1, 4.2 and [51, 54], the equality $I_{1;l} = 0$ holds at a zero signal. The character of radiation self-switching and a system sensitivity to variations in the signal and pump waves depend on the parameter u.

According to (4.8.3), the output intensity of the second harmonic for $I_{21;l} = 0$ is estimated by the formula [73]:

$$I_{2;l} \approx I_{10;0}\left(\frac{1-u}{1+u}\right)^2,$$

from which it follows that at $u \ll 1$ nearly all the radiation is concentrated in the second harmonic. When a signal of the power

$$I_{21;0} = I_{21;0\mathrm{M}} \approx (1-u)\frac{128 I_{10;0}}{\cos^2\psi_0^{(q)}}\exp(-2\widetilde{L})\left(1 + q\,\frac{\alpha_2}{2\gamma_2}\right)^{-1}, \qquad (4.8.4)$$

complying with the condition $u = 1$ is coupled into the system input, all the radiation power at the output is concentrated in the first harmonic [73], i.e. output power is transferred from the wave of one frequency to that of another frequency under application of a weak signal to the waveguide input. Notice that when $u > 1$, there exist no signal magnitudes at which all the output radiation possesses the frequency ω. Hence, the condition $u \ll 1$ holds the greatest interest, because just in this event the complete radiation self-switching occurs.

The steepness of the self-switching characteristic at $I_{21;0} \ll I_{21;0\mathrm{M}}$ is defined by the expression [73]:

$$\frac{\mathrm{d}I_{2;l}}{\mathrm{d}I_{21;0}} \approx -\frac{\mathrm{d}I_{1;l}}{\mathrm{d}I_{21;0}} \approx -\frac{(1-u)}{(1+u)^3}\left(1 + q\,\frac{\alpha_2}{2\gamma_2}\right)\frac{\cos^2\psi_0^{(q)}}{32}\exp 2\widetilde{L}\,, \qquad (4.8.5)$$

where $I_{j;l} = |A_{j0}(z=l)|^2 + |A_{j1}(z=l)|^2$, and $\exp\widetilde{L} \gg 1$.

If $\alpha_1 \neq 0$, then we can also control the relationship among intensities of the ω-wave and 2ω-wave at the system output by varying the pump intensity. Sensitivity of the system to a change in the pump intensity is estimated at the zero signal as follows [73]:

$$\frac{\mathrm{d}I_{2;l}}{\mathrm{d}I_{1;0}} \approx -\frac{\mathrm{d}I_{1;l}}{\mathrm{d}I_{1;0}} \approx -\frac{(1-u)}{(1+u)^3}(u^2 + 4\widetilde{L}u - 1)\,. \qquad (4.8.6)$$

Extraordinary interesting result follows from Eqns (4.8.5) and (4.8.6) at u satisfying the condition [73]:

$$u = \sqrt{4\widetilde{L}^2 + 1} - 2\widetilde{L}\,, \qquad (4.8.7)$$

when the optical switch appears to be insensitive (in the first approximation) to the pump change, but it is highly sensitive to the signal variation, i.e. signal gain is estimated from formula (4.8.5) with $u \approx 0$. To put it differently, an optical transistor stable to the pump instability and possessing high gain factor relative to the signal could be developed in this regime. The former is analogous to the optical transistor based on cubically-nonlinear TCOWs and some other UDCWs with a linear coupling coefficient in a cubically-

nonlinear medium, which has been described earlier in Refs [1, 52, 55 – 57, 62].

Expediency of employing TCOWs for the purpose of development of optical switches and transistors considered in Refs [51, 53] and in Sections 4.2, 4.3 above has been stressed still in first publications [51, 53]. Some specific features of that self-switching event were examined in Refs [70, 73] and in the present section.

Just the same radiation self-switching from one frequency to the other was described by Stegeman and coworkers [120] six years after our publications [51, 53]. Whilst their work formally concerned the situation with light self-switching from one frequency to another in tunnel-coupled optical waveguides (TCOW), and yet the peculiarities of such switching (resulted exactly from the use of TCOWs) were not taken into account, as conditions of the 'coupled-wave synchronism' (CWS, see Section 4.7) were not in use. Therefore, graphs dealing with output intensities in Ref. [120] coincide in essence with those from the article [53] (see Fig. 15). In Ref. [120], synchronism was attained through modulation of a quadratic nonlinearity.

Giving a report at the CLEO '96 conference in Anaheim, CA in June 1996, Stegeman† related the regenerated interest in second harmonic generation to new possibilities for construction of all-optical switches. He cited his still unpublished work and anew failed to mention (hushed up) our publications on this subject [51, 53].

5. Logic elements

With the availability of optical transistors it will be simple in concept to construct on their base some optical logic elements capable of performing arithmetic and logic operations [134, 135]. These elements have to feature two well-defined states '0' and '1' with switching in between which is realized under application of a small signal. The type of a logic element, which may be AND or OR, is determined by the relationship between the signal magnitude and the width of the amplification region of an optical transistor.

The TCOW-based and other UDCW-based logic elements [34, 37, 39] depend for their operation on the relationship between the power transfer coefficient for each wave (see Fig. 1 and Ref. [1]) and the signal input intensity: the steep region (with very large gain $k_s \gg 1$) gives way to a slanting one (where $k_s \sim 0$) and the self-switch at hand operates as a pulse limiter for intensity with existence of two well-defined states '0' and '1'. The middle switching point M_1 can be adopted for the state '1', where $T_1 = 1$, whereas the point M_0‡ or the region positioned somewhat righter than this point, where $T_1 \approx 0$, is adopted for the state '0'. Let us assume that the pump wave is such that the system finds itself at the point M_0 without signal coupling into the waveguide. Synchronous with the pump wave, two logic signals of intensity $I_{sa} = I_{sb} = I_s$ are applied to the same waveguide or to the neighbouring one. The TCOW-based logic elements AND and OR [37] differ in relationship between the signal amplitude I_s and the width ΔI of the amplification region for the self-switch, which is estimated by formula (2.2.2) in a particular case (ΔI estimates for other regimes can be found in Ref. [1]). As a rule, the following relationship $I_s \approx \Delta I/2$ is chosen for the logic elements AND, which is why combination of signals at the system input correlates with addition of pump intensities at the output. For the logic element OR, intensities meet the condition $I_s \geqslant \Delta I$, i.e. the input signal intensity 'falls' within the region where a self-switch operates as a pulse limiter [35], and on the signal combination at the waveguide input the coefficient of the power transfer T_1 would remain about the same as though a single signal is applied to the waveguide, i.e. close to unity (see Fig. 1 and Ref. [1]). There is no difficulty in seeing that under this choice of parameters and the proper selection of output power levels (c) compatible with logic levels '0' and '1' (say, $T_1 \leqslant 0.1$ and $T_1 \geqslant 0.9$, respectively) we shall arrive at $I_s \approx \Delta I/2$ when $a = 1, \quad b = 1 \Rightarrow c = 1; \quad a = 0, \quad b = 1 \Rightarrow c = 0; \quad a = 1, \quad b = 0 \Rightarrow c = 0$, i.e. the logic element AND appears, whereas for $I_s \geqslant \Delta I$ we shall have $a = 1, \ b = 1 \Rightarrow c = 1; \ a = 0, \ b = 1 \Rightarrow c = 1; \ a = 1, \ b = 0 \Rightarrow c = 1$, i.e. the logic element OR.

To ensure that output intensities of logic elements do not depend on the input phases of signal and pump waves, we may, for example, adopt the signal polarizations to be orthogonal to each other (their total intensity equals sum of signal intensities) and a pump-wave frequency to be different from a signal frequency (see [41] and Section 5.4 in Ref. [1]).

At the moment perspectiveness of the TCOW-based logic elements advanced in Ref. [37] is universally recognized (see, for instance, Ref. [136]).

6. On the physical meaning of the UDCW self-switching phenomenon

A crude analogy of cubically-nonlinear system with UDCWs to a nonlinear rigid-rod pendulum may help in revealing the physical meaning of this phenomenon. One can say that critical intensity ($I_{00} = I_M$) accords with potential energy of the pendulum turned 'upside down', i.e. its position of unstable equilibrium at the top point with zero velocity at that point. As this takes place, a small variation of initial energy I_{00} gives rise to a large change in the pendulum motion being described by hyperbolic functions. If energy measuring well below critical one ($(I_{00}/I_M)^2 \ll 1$) can be imparted to the pendulum, then it will oscillate in the neighbourhood of the down position of stable equilibrium (a regime close to a linear one). If energy comprising well above critical one ($(I_{00}/I_M)^2 \gg 1$) is imparted to the pendulum, then it will gyrate on the rod periodically passing through a top position. The pendulum motion is described by trigonometric functions in last two cases.

We can likely say that at the middle self-switching point M (when $I_{00} = I_M$) there comes a kind of 'resonance' between distributed coupling specifying the frequency of spatial beats and the nonlinear constraining force. This resonance gives rise to a sharp dependence of a difference in effective phase velocities of the waves (and, consequently, degree of energy transfer in between) on the input intensity.

7. Conclusions

In summary we shall dwell briefly on some prospects for applying optical switches and transistors advanced for the first time in Refs [33, 34] and pioneered in realization in Ref. [45].

† Jäger M, Stegeman G et al., in *Proc. Conference on Lasers and Electro-optics — CLEO '96* (Anaheim, California, June 2 – 7, 1996); *Technical Digest Series* **9** 122 (1996).

‡ The pump wave can be applied both to the input of one waveguide and the inputs of both the waveguides (see [1]).

First, the speed of response typical of such optical elements is crucially superior to switches based on the Fabry–Perot resonators [24, 25] because it is determined by the optical-nonlinearity setting time τ_{nl} rather than the time of field setting in a resonator.

Second, for the most part these devices make optical waveguides and, as known, great power densities can be concentrated on them; in consequence, light switching is possible at relatively small input power.

Third, the devices concerned are free of a powerful reflected wave at the entrance which induces noises; this wave is intrinsic to bistable elements around oppositely directed waves and, in particular, to those with a Fabry–Perot resonator as the base.

Fourth, these devices feature two inputs and two outputs (quadripoles) and thus they are suitable for combining into optically integrated circuits.

And fifth, such switches are more sensitive to a signal variation (being possessed far greater gain factor) as against the competitive waveguide-based switches (say, of the Mach–Zehnder type) and hence the former hold greater promise for constructing optical transistors and amplifiers.

8. Appendix

To attain not only qualitative accord between theory and observation, but qualitative one as well [45], let us allow for above-mentioned intensity averaging over apparatus time τ_a. In doing so we shall count off the height of each pulse possessed by the third train from the lower boundary of a subsequent pulse 'pedestal' (see Figs 8–11). Then electric signals on the oscillograph screen would be expressed [see Eqn (2.2.1)] in terms of the input-signal instantaneous intensity $I_{00}(t) = I_{00}^a \,\mathrm{form}\,(t)$:

$$S_{00} = m_0 S \frac{1}{\tau_a} \int_{-\tau_a/2}^{\tau_a/2} I_{00}(t)\,\mathrm{d}t\,,$$

$$S_{0M} = m_0 S \frac{I_{0M}}{\tau_a} \int_{-\tau_a/2}^{\tau_a/2} \mathrm{form}\,(t)\,\mathrm{d}t\,,$$

$$S_{jl} = m_l S \frac{1}{2\tau_a} \int_{-\tau_a/2}^{\tau_a/2} I_{00}(t) \left\{ 1 + (-1)^j \,\mathrm{cn}\left[L, \frac{I_{00}(t)}{I_{0M}} \right] \right\} \mathrm{d}t\,, \tag{A.1}$$

where $m_0 \approx 4.6\,\mathrm{mV\,W^{-1}}$, $m_{0,l}$ are the coefficients; m_l depends on optical filters *28* (see Fig. 7) and being different for various sets of experiments it comprises $m_l \approx 2.5 m_0$ for the D run; area of the waveguide cross section $S \approx \pi a^2 \approx 5 \times 10^{-8}\,\mathrm{cm^2}$; I_{00}^a is the amplitude of $I_{00}(t)$, and, finally, form (t) defines the pulse profile. For $\tau_a \gg \tau_p$, then integration limits in (A.1) may be considered infinitive.

Figure 12 displays the dependences $S_{jl}(S_{00})$ [70] plotted (for oscillograms in Fig. 11d–f) by the least-squares method in accordance with experimental data and assuming that each ultrashort pulse takes the form [15]:

$$\mathrm{form}\,(t) = \frac{\sin^2(\pi t/\tau_p)}{(\pi t/\tau_p)^2}\,. \tag{A.2}$$

For such pulse profile we have $S_{00} = m_0 I_{00}^a \tau_p/\tau_a$, $S_{0M} = m_0 I_{0M} \tau_p/\tau_a$. Experimental data fit the curves $S_{jl}(S_{00})$ (see Fig. 12) reasonably well. The third pulse train in Fig. 11 correlates with radiation emerged from the zeroth waveguide, while I_{00}^a in Fig. 11d fits the system point M. The following pairs of parameters correspond to the oscillogram in Fig. 11d and some curves in Fig. 12a [70]: $L = (1.63 \pm 0.03)\pi$, $S_{0M} \approx (23.6 \pm 1)$ mW; for Fig. 11e and curves in Fig. 12b — $L = (1.59 \pm 0.03)\pi$, $S_{0M} \approx (22.8 \pm 1)$ mW; for Fig. 11f and curves in Fig. 12c — $L = (1.57 \pm 0.03)\pi$, $S_{0M} = (24 \pm 1)$ mW. If we put $\tau_p/\tau_a \approx 0.1$, then $I_{0M} \approx 10^9\,\mathrm{W\,cm^{-1}}$, which is agree with the estimate submitted in Ref. [37] well before the experiment (and presented in [1]). Knowing $L \approx 1.6\pi$, $K \approx 5 \times 10^{-7}$ is easily obtainable, and given K and I_{0M}, we arrive at values of $\Theta \approx 4 \times 10^{-13}$ esu and $n_2 \approx 1.3 \times 10^{-13}$ esu coinciding in the order of magnitude with tabulated data (see, e.g., [15]) and with observable findings [40] (see Section 3.1).

References

1. Maĭer A A *Usp. Fiz. Nauk* **165** 1037 (1995) [*Phys. Usp.* **38** 991 (1995)]
2. Iogansen L V *Zh. Eksp. Teor. Fiz.* **40** 1838 (1961) [*Sov. Phys. JETP* **13** 1241 (1961)]
3. Zolotov E M, Kiselev V A, Sychugov V A *Usp. Fiz. Nauk* **112** 231 (1974) [*Sov. Phys. Usp.* **17** 64 (1974)]
4. Barnoski M (Ed.) *Introduction to Integrated Optics* (New York: Plenum Press, 1974) [Translated into Russian (Moscow: Mir, 1977)]
5. Tamir T (Ed.) *Integrated Optics* (Heidelberg: Springer-Verlag, 1975)
6. Hunsperger R *Integrated Optics*: *Theory and Technology* (Heidelberg: Springer-Verlag, 1982) [Translated into Russian (Moscow: Mir, 1985)]
7. Yariv A *Quantum Electronics* 2nd edition (New York: Wiley, 1975) [Translated into Russian (Moscow: Sov. Radio, 1980)]
8. Yariv A *Introduction to Optical Electronics* 2nd edition (New York: Holt, Reinhart and Winston, 1976) [Translated into Russian (Moscow: Vysshaya Shkola, 1982)]
9. Marcuse D *Light Transmission Optics* (New York: Van Nostrand, 1972) [Translated into Russian (Moscow: Mir, 1974)]
10. Snyder A W, Love J D *Optical Waveguide Theory* (London: Methuen, 1984) [Translated into Russian (Moscow: Radio i Svyaz', 1987)]
11. Gowar J *Optical Communication Systems* (Englewood Cliffs: Prentice-Hall, 1984) [Translated into Russian (Moscow: Radio i Svyaz', 1989)]
12. Akhmanov S A, Khokhlov R V *Problemy Nelineĭnoĭ Optiki* (Problems of Nonlinear Optics) (Moscow: Nauka, 1964) [Translated into English *Nonlinear Optics* (New York: Gordon and Breach, 1972)]
13. Bloembergen N *Nonlinear Optics*: *A Lecture Note* (New York: Benjamin, 1965) [Translated into Russian (Moscow: Mir, 1966)]
14. Zernike F, Midwinter J E *Applied Nonlinear Optics*: *Basics and Applications* (New York: Wiley Interscience, 1973) [Translated into Russian (Moscow: Mir, 1976)]
15. Akhmanov S A, Vysloukh V A, Chirkin A S *Optika Femtosekundnykh Lazernykh Impul'sov* (Moscow: Nauka, 1988) [Translated into English *Optics of Femtosecond Laser Pulses* (New York: AIP Press, 1992)]
16. Lugovoĭ V N *Zh. Eksp. Teor. Fiz.* **56** 683 (1969) [*Sov. Phys. JETP* **29** 374 (1969)]
17. Seidel H *Bistable Optical Circuit Using Saturable Absorber within a Resonant Cavity* US Patent No. 3610731 (1969)
18. Szöke A et al. *Appl. Phys. Lett.* **15** 376 (1969)
19. Duguay M A, Hansen J W *Appl. Phys. Lett.* **15** 192 (1969)
20. McCall S L, Gibbs H M, Venkatesan T N C *J. Opt. Soc. Am.* **65** 1184 (1975)
21. Gibbs H M, McCall S L, Venkatesan T N C *Phys. Rev. Lett.* **36** 1135 (1976)
22. Kaplan A E *Pis'ma Zh. Eksp. Teor. Fiz.* **24** 132 (1976) [*JETP Lett.* **24** 114 (1976)]
23. Askar'yan G A *Pis'ma Zh. Eksp. Teor. Fiz.* **8** 19 (1968) [*JETP Lett.* **8** 10 (1968)]
24. Felber F S, Marburger J H *Appl. Phys. Lett.* **28** 731 (1976)
25. Marburger J H, Felber F S *Phys. Rev. A* **17** 335 (1978)

26. Okuda M, Onaka K *Jpn. J. Appl. Phys.* **16** 769 (1977)
27. Winful H G, Marburger J H, Garmire E *Appl. Phys. Lett.* **35** 379 (1979)
28. Winful H G, Marburger J H *Appl. Phys. Lett.* **36** 613 (1980)
29. Kukhtarev N V, Semenets T I *Kvantovaya Elektron.* (Moscow) **8** 2005 (1981) [*Sov. J. Quantum Electron.* **11** 1216 (1981)]
30. Kukhtarev N V, Semenets T I *Zh. Tekh. Fiz.* **51** 1990 (1981) [*Sov. Phys. Tech. Phys.* **26** 1159 (1981)]
31. Lugovoĭ V N *Kvantovaya Elektron.* (Moscow) **6** 2053 (1979) [*Sov. J. Quantum Electron.* **9** 1207 (1979)]
32. Gibbs H M *Optical Bistability: Controlling Light with Light* (New York: Academic Press, 1985) [Translated into Russian (Moscow: Mir, 1988)]
33. Maĭer A A *Sposob Pereklyucheniya Signala v Tunnel'no-Svyazannykh Opticheskikh Volnovodakh* (Method for Signal Switching in Tunnel-Coupled Optical Waveguides) USSR Patent No. 1152397 (1982) (appl. 1982, publ. 1988); *Byull. Izobret.* (46) 300 (1988)
34. Maĭer A A "Optical transistors and bistable elements based on nonlinear light transmission by the systems with unidirectional coupled waves" *Kvantovaya Elektron.* (Moscow) **9** 2296 (1982) [*Sov. J. Quantum Electron.* **12** 1490 (1982)]
35. Maĭer A A *Kvantovaya Elektron.* (Moscow) **11** 157 (1984) [*Sov. J. Quantum Electron.* **14** 101 (1984)]
36. Jensen S M *IEEE J. Quantum Electron.* **QE-18** 1580 (1982)
37. Maĭer A A *Izv. Akad. Nauk SSSR Ser. Fiz.* **48** 1441 (1984) [*Bull. Acad. Sci. USSR Ser. Phys.* **48** 192 (1984)]
38. Maĭer A A, Preprint IOFAN No. 236 (Moscow: Institute of General Physics, USSR Academy of Sciences, 1984); *Kvantovaya Elektron.* (Moscow) **12** 1537 (1985) [*Sov. J. Quantum Electron.* **15** 1016 (1985)]
39. Maĭer A A *Kratk. Soobshch. Fiz.* (12) 20 (1984)
40. Gusovskiĭ D D, Dianov E M, Maĭer A A et al. Preprint IOFAN No. 250-13 (Moscow: Institute of General Physics, USSR Academy of Sciences, 1984); *Kvantovaya Elektron.* (Moscow) **12** 2312 (1985) [*Sov. J. Quantum Electron.* **15** 1523 (1985)]
41. Maĭer A A, Preprint IOFAN No. 122-26 (Moscow: Institute of General Physics, USSR Academy of Sciences, 1985); *Kvantovaya Elektron.* (Moscow) **13** 1360 (1986) [*Sov. J. Quantum Electron.* **16** 892 (1986)]
42. Maĭer A A , Sitarskiĭ K Yu, Preprint IOFAN No. 311-20 (Moscow: Institute of General Physics, USSR Academy of Sciences, 1985); *Kvantovaya Elektron.* (Moscow) **14** 1604 (1987) [*Sov. J. Quantum Electron.* **17** 1018 (1987)]
43. Maĭer A A, Preprint IOFAN No. 334-20 (Moscow: Institute of General Physics, USSR Academy of Sciences, 1985); *Kvantovaya Elektron.* (Moscow) **14** 1596 (1987) [*Sov. J. Quantum Electron.* **17** 1013 (1987)]
44. Maĭer A A, Preprint IOFAN No. 276 (Moscow: Institute of General Physics, USSR Academy of Sciences, 1986); *Kratk. Soobshch. Fiz.* (9) 43 (1986)
45. Gusovskiĭ D D, Dianov E M, Maĭer A A et al. "Experimental evidence of light self-switching in tunnel-coupled optical waveguides", Preprint IOFAN No. 188 (Moscow: Institute of General Physics, USSR Academy of Sciences, 1986); Paper presented at International Seminar 'Optical Computing – 86', Novosibirsk, July 1986 [In March 1987, Prof. W Rhodes (Editor of Applied Optics) summarized the results of Refs [34, 35, 37, 45] in a report: Bill Rhodes 'Alexander Mayer's papers on nonlinear optical switching in coupled waveguides' presented at the OSA Optical Computing Conference held in March 1987 at Lake Tahoe (Incline Village), NV. Prof. Rhodes sent out reprints of the article [45] in English to many foreign scientists]; *Kvantovaya Elektron.* (Moscow) **14** 1144 (1987) [*Sov. J. Quantum Electron.* **17** 742 (1987)]
46. Maĭer A A, Serdyuchenko Yu N, Sitarskiĭ K Yu et al. Preprint IOFAN No. 345 (Moscow: Institute of General Physics, USSR Academy of Sciences, 1986); Paper presented at International Seminar 'Optical Computing – 86', Novosibirsk, July 1986; *Kvantovaya Elektron.* (Moscow) **14** 1157 (1987) [*Sov. J. Quantum Electron.* **17** 735 (1987)]
47. Maĭer A A, Preprint IOFAN No. 43-20 (Moscow: Institute of General Physics, USSR Academy of Sciences, 1987)
48. Maĭer A A, Preprint IOFAN No. 62-10 (Moscow: Institute of General Physics, USSR Academy of Sciences, 1987); *Kratk. Soobshch. Fiz.* (6) 58 (1987)
49. Maĭer A A, Preprint IOFAN No. 153-26 (Moscow: Institute of General Physics, USSR Academy of Sciences, 1987)
50. Maĭer A A, Sitarskiĭ K Yu "Sposob Upravleniya Koeffitsientom Preobrazovaniya Moshchnosti Izlucheniya s Odnoĭ Chastoty na Druguyu" (Method for Controlling the Coefficient of Radiation Power Conversion from One Frequency to Another) USSR Author's Certificate No. 1593438 (appl. 1987, recorded in the State Register 15 May 1990)
51. Maĭer A A, Sitarskiĭ K Yu *Kvantovaya Elektron.* (Moscow) **14** 2369 (1987) [*Sov. J. Quantum Electron.* **17** 1507 (1987)]; "Radiation switching from one frequency to the other in a quadratically nonlinear medium and the optical transistor on its base", Preprint IOFAN No. 222 (Moscow: Institute of General Physics, USSR Academy of Sciences, 1987)
52. Maĭer A A, Preprint IOFAN No. 351-45 (Moscow: Institute of General Physics, USSR Academy of Sciences, 1987)
53. Maĭer A A, Sitarskiĭ K Yu *Dokl. Akad. Nauk SSSR Ser. Fiz.* **299** 1387 (1988) [*Sov. Phys. Dokl.* **33** 293 (1988)]; "Optical transistor and switch based on a parametric two-frequency interaction in a quadratically nonlinear medium", Preprint IOFAN No. 314 (Moscow: Institute of General Physics, USSR Academy of Sciences, 1987)
54. Maĭer A A, Sitarskiĭ K Yu, Preprint IOFAN No. 111-29 (Moscow: Institute of General Physics, USSR Academy of Sciences, 1988)
55. Maĭer A A *Dokl. Akad. Nauk SSSR Ser. Fiz.* **303** 618 (1988); [*Sov. Phys. Dokl.* **33** 852 (1988)]
56. Maĭer A A, in *Proceedings of Third International Conference Trends in Quantum Electronics '88* (Bucharest, 1988) p. 382
57. Maĭer A A *Papers on Optical Communication* (Special Issue) (Bellingham, WA: Society of Photo-Optical Instrumentation Engineers — International Society for Optical Engineering, 1988) p. 27
58. Maĭer A A, Sitarskiĭ K Yu, Preprint IOFAN No. 86-23 (Moscow: Institute of General Physics, USSR Academy of Sciences, 1989); *Dokl. Akad. Nauk SSSR Ser. Fiz.* **307** 592 (1989) [*Sov. Phys. Dokl.* **34** 644 (1989)]
59. Maĭer A A, Karataev S G, Preprint IOFAN No. 73-7 (Moscow: Institute of General Physics, USSR Academy of Sciences, 1989); *Dokl. Akad. Nauk SSSR Ser. Fiz.* **309** 619 (1989) [*Sov. Phys. Dokl.* **34** 1025 (1989)]
60. Dianov E M, Kuznetsov A V, Maĭer A A et al. *Dokl. Akad. Nauk SSSR Ser. Fiz.* **309** 611 (1989) [*Sov. Phys. Dokl.* **34** 1021 (1989)]
61. Dianov E M, Kuznetsov A V, Maĭer A A et al. *Opt. Commun.* **74** 152 (1989)
62. Maĭer A A, in *Proceedings of OSA Photonic Switching Conference, Salt Lake City, 1989* (Vol. 3 of OSA Proceedings Series) (Washington, DC: Optical Society of America, 1989) p. 85
63. Maĭer A A "Nonlinear interaction of unidirectional distributively coupled waves", Thesis for Doctorate of Physicomathematical Sciences (Moscow: Institute of General Physics, USSR Academy of Sciences, 1990)
64. Maĭer A A "Opticheskiĭ mul'tivibrator" (Optical Multivibrator) USSR Patent No. 2003150 (1990)
65. Maĭer A A "Opticheskiĭ mul'tivibrator" (Optical Multivibrator) USSR Author's Certificate No. 1805437 (1990)
66. Maĭer A A *Dokl. Akad. Nauk SSSR Ser. Fiz.* **315** 95 (1990) [*Sov. Phys. Dokl.* **35** 947 (1990)]
67. Maĭer A A, Preprint IOFAN No. 40-30 (Moscow: Institute of General Physics, USSR Academy of Sciences, 1991); *Kvantovaya Elektron.* (Moscow) **18** 1447 (1991) [*Sov. J. Quantum Electron.* **21** 1334 (1991)]
68. Maĭer A A, Preprint IOFAN No. 42-13 (Moscow: Institute of General Physics, USSR Academy of Sciences, 1991); *Kvantovaya Elektron.* (Moscow) **18** 1264 (1991) [*Sov. J. Quantum Electron.* **21** 1148 (1991)]
69. Maĭer A A, Karataev S G, Preprint No. 46 (Moscow: Institute of General Physics, Academy of Sciences of the USSR, 1991); Maĭer A A, Sitarskiĭ K Yu *Kvantovaya Elektron.* (Moscow) **23** 167 (1996) [*Quantum Electron.* **26** 163 (1996)]
70. Sitarskiĭ K Yu "Nonlinear interaction of waves in tunnel-coupled optical waveguides", Thesis for Candidate of Physicomathematical Sciences (Moscow: Institute of General Physics, USSR Academy of Sciences, 1990)
71. Maĭer A A, Preprint IOFRAN No. 30 (Moscow: Institute of General Physics, RF Academy of Sciences, 1992)

72. Maĭer A A, Sitarskiĭ K Yu *Dokl. Akad. Nauk RF Ser. Fiz.* **337** 597 (1994) [*Phys.- Dokl.* **39** 558 (1994)]
73. Maĭer A A, Sitarskiĭ K Yu, Preprint IOFRAN No. 27 (Moscow: Institute of General Physics, RF Academy of Sciences, 1995)
74. Kitayama K, Wang S *Appl. Phys. Lett.* **43** 17 (1983)
75. Kitayama K, Kimura Y, Seikai S *Appl. Phys. Lett.* **46** 317 (1985)
76. Li Kam Wa P et al. *Electron. Lett.* **21** 26 (1985)
77. Daino B, Gregori G, Wabnitz S *J. Appl. Phys.* **58** 4512 (1985)
78. Daino B, Gregori G, Wabnitz S *Opt. Lett.* **11** 42 (1986)
79. Winful H G *Opt. Lett.* **11** 33 (1986)
80. Hoffe R, Chrostowski J *Opt. Commun.* **57** 34 (1986)
81. Trillo S, Wabnitz S *Appl. Phys. Lett.* **49** 752 (1986)
82. Snyder A W et al. *Opt. Lett.* **15** 357 (1990)
83. Wabnitz S et al. *Appl. Phys. Lett.* **49** 838 (1986)
84. Trillo S et al. *Appl. Phys. Lett.* **49** 1224 (1986)
85. Mecozzi A et al. *Opt. Lett.* **12** 275 (1987)
86. Caglioti E, Trillo S, Wabnitz S *Opt. Lett.* **12** 1044 (1987)
87. Das U, Chen Y, Bhattacharya P *Appl. Phys. Lett.* **51** 1679 (1987)
88. Trillo S, Wabnitz S *J. Opt. Soc. Am. B* **5** 483 (1988)
89. Chen Y, Snyder A W *Opt. Lett.* **14** 1237 (1989)
90. Trillo S et al. *Appl. Phys. Lett.* **53** 837 (1988)
91. Friberg S R, Smith P W *IEEE J. Quantum Electron.* **QE-23** 2089 (1987)
92. Friberg S R et al. *Appl. Phys. Lett.* **51** 1135 (1987)
93. Friberg S R et al. *Opt. Lett.* **13** 904 (1988)
94. Cada M et al. *Appl. Phys. Lett.* **49** 755 (1986)
95. Berger P et al. *Appl. Phys. Lett.* **52** 1125 (1988)
96. Jin R et al. *Appl. Phys. Lett.* **53** 1791 (1988)
97. Silberberg Y et al. *Appl. Phys. Lett.* **46** 701 (1985)
98. Park H G, Huang S Y, Kim B Y *Opt. Lett.* **14** 877 (1989)
99. Caglioti E et al. *J. Opt. Soc. Am. B* **5** 472 (1988)
100. Finlayson N, Stegeman G I *Appl. Phys. Lett.* **56** 2276 (1990)
101. Schmidt-Hattenberger C, Trutschel U, Lederer F *Opt. Lett.* **16** 294 (1991)
102. Schmidt-Hattenberger C et al. *Opt. Quantum Electron.* **24** 691 (1992)
103. Mitchell D J, Snyder A W, Chen Y *Electron. Lett.* **26** 1164 (1990)
104. Petrov M P, Kuzin E A, Maksyutenko M A *Kvantovaya Elektron.* (Moscow) **18** 1395 (1991) [*Sov. J. Quantum Electron.* **21** 1282 (1991)]
105. Andrushko L M, Karplyuk K S, Ostrovskiĭ S B *Radiotekh. Elektron.* **32** (2) 427 (1987) [*Sov. J. Commun. Technol. Electron.* **32** 161 (1987)]
106. Trillo S et al. *Opt. Lett.* **13** 672 (1988)
107. Abdullaev F Kh, Abrarov R M, Darmanyan S A *Opt. Lett.* **14** 131 (1989)
108. Wright E M, Stegeman G I, Wabnitz S *Phys. Rev. A* **40** 4455 (1989)
109. Dianov E M, Nikonova Z S, Serkin V N *Kratk. Soobshch. Fiz.* (12) 17 (1989)
110. Trillo S, Wabnitz S *Opt. Lett.* **16** 1 (1991)
111. Soto-Crespo J M, Wright E M *J. Appl. Phys.* **70** 7240 (1991)
112. Maĭmistov A I *Kvantovaya Elektron.* (Moscow) **18** 758 (1991) [*Sov. J. Quantum Electron.* **21** 687 (1991)]
113. Aceves A B, Wabnitz S *Opt. Lett.* **17** 25 (1992)
114. Abdullaev F Kh et al. *Zh. Tekh. Fiz.* **64** 101 (1994)
115. Menyuk C R *Opt. Lett.* **12** 614 (1987)
116. Islam M N, UK Patent Application GB 2249648 A (Priority data 07.11.1990)
117. Maĭer A A, Shklovskiĭ E I *Metod Vvoda Izlucheniya v Opticheskiĭ Volnovod* (Method for Radiation Coupling into Optical Waveguide) USSR Author's Certificate No. 1238569 (app. 1984); *Byull. Izobret.* (29) (1988)
118. Belashenkov N R, Gagarskiĭ S V, Inochkin M V *Opt. Spektrosk.* **66** 1383 (1989) [*Opt. Spectrosc.* **66** 806 (1989)]
119. Stegeman G et al. *Opt. Lett.* **18** 13 (1993)
120. Assanto G et al. *Appl. Phys. Lett.* **62** 1323 (1993)
121. Laureti Palma A et al. "All-optical processing in quadratic nonlinear media", in *Proc. 20-th European Conference on Optical Communication* (*Firenze, Italy, September 25–29, 1994*)
122. Kozhevnikova N N, Thesis for Candidate of Physicomathematical Sciences (Moscow: Institute of General Physics, USSR Academy of Sciences, 1987); *Kratk. Soobshch. Fiz.* (11) 12 (1986)
123. Petrov M P, Kuzin E A, Preprint LFTI No. 975 (Leningrad: Ioffe Physicotechnical Institute, USSR Academy of Sciences, 1985)
124. Maĭer A A *Abstracts IX-th All-Union Conference on Coherent and Nonlinear Optics, Leningrad, 13–16 June, 1978* Part 1 (Moscow, 1978) p. 43
125. Maĭer A A, Sukhorukov A P *Zh. Eksp. Teor. Fiz.* **77** 1282 (1979) [*Sov. Phys. JETP* **50** 645 (1979)]
126. Maĭer A A *Kvantovaya Elektron.* (Moscow) **7** 1596 (1980) [*Sov. J. Quantum Electron.* **10** 925 (1980)]
127. Maĭer A A, Sukhorukov A P *Izv. Akad. Nauk SSSR Ser. Fiz.* **45** 934 (1981) [*Bull. Acad. Sci. USSR Ser. Phys.* **45** 34 (1981)]
128. Maĭer A A *Kvantovaya Elektron.* (Moscow) **9** 2544 (1982) [*Sov. J. Quantum Electron.* **12** 1661 (1982)]
129. Maĭer A A et al. *Kratk. Soobshch. Fiz.* (2) 25 (1983)
130. Stegeman G I, Seaton C T *J. Appl. Phys.* **58** R57 (1985)
131. Bozhevol'nyĭ S I et al. *Pis'ma Zh. Tekh. Fiz.* **7** 649 (1981) [*Sov. Tech. Phys. Lett.* **7** (6) (1981)]
132. Philips N V *Waveguide device with controlled gap* European Patent No. 0430361 (Priority data 23.11.1990) (The earliest priority 30.11.1989 of US Patent No. 445075) Published 05.06.1991; BA Eindhoven, NL
133. Maĭer A A *Kvantovaya Elektron.* (Moscow) **19** 1224 (1992) [*Sov. J. Quantum Electron.* **22** 1147 (1992)]
134. Morozov V N *Optoelektronnye Matrichnye Protsessory* (Optoelectronic Matrix Processors) (Moscow: Radio i Svyaz', 1986)
135. Abraham E, Seaton C T, Smith S D *Sci. Am.* **248** 85 (1983)
136. Maĭmistov A I *Kvantovaya Elektron.* (Moscow) **22** 1044 (1995) [*Quantum Electron.* **25** 1009 (1995)]
137. Lattes A et al. *IEEE J. Quantum Electron.* **QE-19** 1718 (1983)